
Delayed Choice Lorentz Transformations on a Qubit

Lucas Burns, Sacha Greenfield, Justin Dressel

Abstract A continuously monitored quantum bit (qubit) exhibits competition between unitary Hamiltonian dynamics and non-unitary measurement-collapse dynamics, which for diffusive measurements form an enlarged transformation group equivalent to the Lorentz group of spacetime. We leverage this equivalence to develop a four-dimensional generalization of the three-dimensional Bloch ball to visualize the state of a monitored qubit as the four-momentum of an effective classical charge affected by a stochastic electromagnetic force field. Unitary qubit dynamics generated by Hermitian Hamiltonians correspond to elliptic spatial rotations of this effective charge while non-unitary qubit dynamics generated by non-Hermitian Hamiltonians or stochastic measurement collapse correspond to hyperbolic Lorentz boosts. Notably, to faithfully emulate the stochastic qubit dynamics arising from continuous qubit measurement, the stochastic electromagnetic fields must depend on the velocity of the charge they are acting on. Moreover, continuous qubit measurements admit a dynamical delayed choice effect where a future experimental choice can appear to retroactively determine the type of past measurement backaction, so the corresponding point charge dynamics can also exhibit delayed choice Lorentz transformations in which a future experimental choice determines whether stochastic force fields are electric or magnetic in character long after they interact with the particle.

Contents

1	Introduction	2
2	Qubits, Measurement, and Trajectories	3
3	Kinematical Correspondence	8
4	Dynamical Correspondence	10
5	Stochastic Correspondence	15
6	Delayed Choice Lorentz Transformations	21
7	Conclusion	27

L. Burns, S. Greenfield, J. Dressel
 Institute for Quantum Studies,
 Schmid College of Science and Technology,
 Chapman University, Orange CA 92866, USA.

S. Greenfield
 Center for Quantum Information Science and Technology,
 Department of Physics and Astronomy,
 University of Southern California, Los Angeles, CA 90089, USA.

1 Introduction

Recent experimental progress in quantum hardware has enabled concurrent monitoring of quantum state evolution, highlighting the inherent tension between unitary Hamiltonian dynamics and non-unitary measurement-collapse dynamics. Unlike typical prepare-and-measure scenarios that relegate the use of measurement solely to the beginning and end of an experimental protocol, monitoring the state evolution irreducibly interleaves Hamiltonian dynamics with measurement-collapse dynamics to produce *conditioned quantum state trajectories* as the most complete description of the system given the monitored record [1–16]. Superconducting quantum processors in particular have demonstrated a range of utility for such quantum trajectories, including to monitor quantum jumps [17–20], passively track diffusive dynamics [21–28], actively control dynamics with feedback [29–39], remotely generate entanglement [40, 41], and continuously check syndromes for error correction [42–45].

The effective dynamics resulting from such concurrent monitoring are fundamentally non-unitary and stochastic, with a richer mathematical structure than standard unitary quantum dynamics. In the ideal case, efficiently monitoring a quantum system (i.e., with no dissipative information loss) produces evolution generated by stochastic non-Hermitian Hamiltonians that can have interesting properties not shared by Hermitian Hamiltonians [46–54]. Indeed, the recent interest in engineering quasi-deterministic non-Hermitian Hamiltonians [55] (e.g., via post-selection on a sequence of no-jump results given a monitoring process with rare jumps [56–61]) is a special case of such monitored evolution that underscores the potential benefits of studying the enlarged class of transformations inherent to monitored dynamics.

For the case of diffusive monitoring, which is the standard readout protocol for superconducting circuits [13–15], each observation in a temporal sequence yields a non-projective (weak) measurement transformation [62, 63] on the state that is technically invertible with a complementary observation, implying that the enlarged class of monitored dynamics still forms a (non-unitary) transformation group. The lower likelihood of observing inverse transformations produces the apparent statistical arrow of time that favors collapse toward measurement eigenstates on average while retaining invertibility [64]. Focusing on qubits as the simplest non-trivial quantum system, the class of transformations for such diffusively monitored dynamics widens from the special unitary group $SU(2)$ to the special linear group $SL(2, \mathbb{C})$ [65]. However, this enlarged group representation is contingent on using the state norm to partially track the accumulated probability for the observed measurement record, such that the number of independent real parameters needed to characterize the qubit state increases from 3 to 4. This extra parameter is problematic for the traditional Bloch ball visualization of a qubit, which assumes a normalized state that can be identified with a 3-dimensional spin-vector. Thus, traditional analyses of monitored qubit dynamics have renormalized the state after each observation to yield nonlinear dynamics that restore the viability of the Bloch ball visualization at the cost of obfuscating the enlarged group structure.

In this paper, we generalize the 3-dimensional Bloch ball to a 4-dimensional representation that accommodates the enlarged group structure of monitored qubit dynamics. We find that this 4-dimensional representation naturally has the Lorentz group structure of spacetime, which may be somewhat surprising since an abstract qubit has no connection to spacetime *a priori*. Nevertheless, the enlarged general linear group $SL(2, \mathbb{C})$ of monitored qubit dynamics is equivalent to a matrix representation of the Lorentz group of spacetime transformations suitable for Weyl spinors [66] and twistors [67], and naturally relates to Clifford-algebraic treatments of spacetime symmetries [68–75]. As such, our representation yields a precise correspondence between the four real components of the unnormalized qubit state and the components of a proper four-momentum for a point charge in spacetime (and generalizes Ref. [76]). The three-dimensional Bloch vector obtained after renormalization then corresponds to the three-velocity of that point charge in a particular frame, providing an intriguing perspective on the significance of state renormalization during monitoring. With this spacetime representation, the enlarged group of stochastic dynamics for the monitored qubit state intuitively corresponds to the dynamics of a spacetime point charge being influenced by stochastic electro-

magnetic force fields [77–80], which gives a concrete and familiar way to visualize monitored qubit dynamics beyond the Bloch ball. Magnetic fields correspond to Hermitian generators of elliptic (unitary) dynamics producing spatial rotations of the charge, while electric fields correspond to anti-Hermitian generators of hyperbolic (measurement-collapse) dynamics producing linear boosts of the charge.

Much like one can interpret the three-dimensional Bloch vector representation of a normalized qubit state as a classical spin hidden variable model, one can also interpret our generalization to a spacetime point charge as a concrete classical hidden variable model for a monitored quantum state. One thus expects that any nonclassical features of a qubit should manifest as strange features of its corresponding spacetime charge. We show that the stochastic dynamics of a monitored qubit indeed have several strange features that one would not expect for a truly classical charge in spacetime. First, the corresponding stochastic electromagnetic fields that influence the charge motion must depend on the velocity of the charge they are acting on to reproduce the behavior of measurement collapse. Such a velocity-dependent external field is a form of fine-tuned and instantaneous feedback control that would be highly unusual and difficult to experimentally arrange for an actual point charge. Second, more detailed analysis of how the qubit measurement occurs reveals an intrinsically retrocausal character hidden in the controllable parameters of the corresponding force fields [6]: both the type of electromagnetic field and their specific fluctuations can be determined at later times than their interaction with the charge. In particular, an experimenter is free to vary an angle $\theta(t)$ that determines the type of electromagnetic field, and thus the type of Lorentz transformation, which affects the charge at an earlier interaction time $t - \delta t_q$. Such a dynamical delayed choice effect results from the entanglement of the qubit with the detecting apparatus and thus cannot be replicated by causal electromagnetic fields affecting a truly classical charge. Our four-dimensional representation for the state of a monitored qubit thus not only serves as a useful visualization that preserves the natural group structure of its dynamics, but also helps clarify which features of those dynamics have nonclassical character. In this way our qubit representation is similar in spirit to other toy models that have been used to identify specific nonclassical features through contrast, such as Bell-nonlocality [81–83], Leggett-Garg invasive measurability [84–88], and contextuality [26, 89–91].

The paper is organized as follows: In Section 2, we briefly review how to model quantum state trajectories for a qubit. In Section 3, we develop the kinematical correspondence between a point charge in spacetime and an unnormalized qubit state. In Section 4, we examine the deterministic dynamics of a classical point charge and show the equivalence between the electromagnetic Lorentz force and the non-Hermitian dynamics of an unnormalized qubit state. In Section 5, we examine the stochastic dynamics of a point charge in a fluctuating electromagnetic field and highlight the unusual constraints on the fields that are required to achieve correspondence with the stochastic dynamics of a monitored qubit. In Section 6, we give a more detailed derivation of the measurement process for a superconducting qubit to highlight the delayed choice nature of the effective measurement parameters and the implications for the corresponding stochastic electromagnetic fields affecting its analogous point charge. We conclude in Section 7.

2 Qubits, Measurement, and Trajectories

To establish the foundation for a formal correspondence between point charge and qubit, we first review the mathematical framework of state transformations and measurement trajectories. Here we focus on two-level (qubit) systems, for which normalized pure states have a complex vector representation,

$$|\psi\rangle = c_0 |0\rangle + c_1 |1\rangle, \quad c_0, c_1 \in \mathbb{C}, \quad \langle\psi|\psi\rangle = 1, \quad (1)$$

and for which normalized convex mixtures $\hat{\rho} = \sum_m p_m |\psi_m\rangle\langle\psi_m|$ with $p_m \in [0, 1]$ such that $\sum_m p_m = 1$, have a matrix representation,

$$\hat{\rho} = \frac{1}{2} \left(\hat{1} + \sum_{k=1}^3 S_k \hat{\sigma}_k \right), \quad \text{Tr}(\hat{\rho}) = 1, \quad S_k = \text{Tr}(\hat{\sigma}_k \hat{\rho}) \in \mathbb{R}, \quad (2)$$

in terms of the Pauli matrices defined as

$$\hat{1} = \hat{\sigma}_0 = |0\rangle\langle 0| + |1\rangle\langle 1|, \quad \hat{\sigma}_x = \hat{\sigma}_1 = |0\rangle\langle 1| + |1\rangle\langle 0|, \quad (3a)$$

$$\hat{\sigma}_y = \hat{\sigma}_2 = -i(|0\rangle\langle 1| - |1\rangle\langle 0|), \quad \hat{\sigma}_z = \hat{\sigma}_3 = |0\rangle\langle 0| - |1\rangle\langle 1|. \quad (3b)$$

The Pauli operator expectation values S_k fully parametrize a mixed state as components of an effective spin (Bloch) vector $\vec{S} = (S_1, S_2, S_3) \in \mathbb{R}^3$ satisfying $|\vec{S}|^2 \leq 1$, making a general normalized qubit state space equivalent to a filled three-dimensional unit (Bloch) ball.

Quantum states in the Schrödinger picture undergo two fundamental types of transformations: (i) unitary Hamiltonian evolution, and (ii) non-unitary collapse from measurement backaction. Unitary transformations satisfy $\hat{U}\hat{U}^\dagger = \hat{U}^\dagger\hat{U} = \hat{1}$ and take the form

$$\hat{U} = \exp \left[-i \left(\phi_0 \hat{1} + \sum_{k=1}^3 \phi_k \hat{\sigma}_k \right) / 2 \right], \quad |\psi\rangle \mapsto \hat{U} |\psi\rangle, \quad \hat{\rho} \mapsto \hat{U} \hat{\rho} \hat{U}^\dagger, \quad (4)$$

where $\phi_\mu \in \mathbb{R}$ for $\mu = 0, 1, 2, 3$. Since ϕ_0 changes only the global phase, it is a gauge freedom for an isolated qubit, so is usually omitted. For an efficient measurement (i.e., without information loss) of a particular result r of a detector, the quantum state transforms according to the non-unitary collapse backaction

$$|\psi\rangle \mapsto \frac{\hat{M}_r |\psi\rangle}{\sqrt{p(r)}}, \quad \hat{\rho} \mapsto \frac{\hat{M}_r \hat{\rho} \hat{M}_r^\dagger}{p(r)}, \quad (5)$$

where

$$p(r) = \langle \psi | \hat{M}_r^\dagger \hat{M}_r | \psi \rangle, \quad p(r) = \text{Tr}(\hat{M}_r^\dagger \hat{M}_r \hat{\rho}), \quad (6)$$

is the probability of the result $r \in R$. To ensure probability normalization $\int_R dr p(r) = 1$, the measurement (Kraus) operators \hat{M}_r satisfy the completeness relation $\int_R dr \hat{M}_r^\dagger \hat{M}_r = \hat{1}$, making $dr \hat{P}_r \equiv dr \hat{M}_r^\dagger \hat{M}_r$ a positive operator-valued measure (POVM) over the detector result index $r \in R$.

This measurement collapse can be understood as a quantum generalization of Bayes' rule [14, 15, 63]. For specificity, consider a measurement in the $\hat{\sigma}_z$ basis. The simplest Bayesian update of the state $|\psi\rangle = \sqrt{p(0)}|0\rangle + \sqrt{p(1)}e^{i\varphi}|1\rangle$ given a measured result r is described by a measurement operator of the form

$$\hat{M}_r = \sqrt{p(r|0)}|0\rangle\langle 0| + \sqrt{p(r|1)}|1\rangle\langle 1| \quad (7)$$

where $p(r|0)$ and $p(r|1)$ are the empirical detector response likelihoods for obtaining the result r given definite preparations of $|0\rangle$ and $|1\rangle$ states, respectively, ensuring that updated probabilities in the normalized post-measurement state adhere to Bayes' rule,

$$|\psi_r\rangle = \frac{\hat{M}_r |\psi\rangle}{\|\hat{M}_r |\psi\rangle\|} = \sqrt{p(0|r)}|0\rangle + \sqrt{p(1|r)}e^{i\varphi}|1\rangle, \quad p(k|r) = \frac{p(r|k)p(k)}{p(r|0)p(0) + p(r|1)p(1)}. \quad (8)$$

Notably, the measurement operator in Eq. (7) can be written in the form,

$$\hat{M}_r = \sqrt{\bar{p}(r)} \exp(\hat{\sigma}_z \lambda(r)/4), \quad \bar{p}(r) \equiv \sqrt{p(r|0)p(r|1)}, \quad \lambda(r) \equiv \ln \frac{p(r|0)}{p(r|1)}, \quad (9)$$

involving the geometric mean $\bar{p}(r)$ of the detector likelihoods and the surprisal difference $\lambda(r)$ [92]. The mean likelihood $\bar{p}(r)$ is largest at maximal overlap and smallest at minimal overlap, bounded above by the largest and below by the smallest of the two probabilities, and it can be understood as a measure of indistinguishability. In contrast, the surprisal difference $\lambda(r)$ is the logarithmic Bayes factor, a signed measure of distinguishability that fully determines the measurement backaction on the state. The limits of $\lambda(r) \rightarrow \pm\infty$ are projective measurements, while $\lambda(r) \approx 0$ are weak measurements [62], and other values of $\lambda(r)$ are generalized measurements of intermediate strength [93]. The mean likelihood $\bar{p}(r)$ contributes a trivial global rescaling of the state and cancels in the renormalization.

To simplify the description of the measurement operator, we use a different normalization convention that keeps only the essential information $\lambda(r)$ in the operator and tracks the mean likelihood $\bar{p}(r)$ as part of the probability definition separately,

$$\hat{L}_r \equiv \frac{\hat{M}_r}{\sqrt{\bar{p}(r)}}, \quad |\tilde{\psi}_r\rangle \equiv \hat{L}_r |\psi\rangle, \quad \hat{s}_r \equiv \hat{L}_r \hat{\rho} \hat{L}_r^\dagger. \quad (10)$$

This choice of scaling retains minimal information in a linear update to an unnormalized conditioned state, $|\tilde{\psi}_r\rangle$ or \hat{s}_r , while still allowing recovery of the measurement probability,

$$p(r) = \bar{p}(r) \langle \tilde{\psi}_r | \tilde{\psi}_r \rangle, \quad p(r) = \bar{p}(r) \text{Tr}(\hat{s}_r), \quad (11)$$

using both the state norm and the separately tracked mean likelihood $\bar{p}(r)$. The trace of the unnormalized state after a single measurement update is

$$\text{Tr}(\hat{s}_r) = \frac{p(r)}{\bar{p}(r)} = e^{\lambda(r)/2} p(0) + e^{-\lambda(r)/2} p(1), \quad (12)$$

which tells us how informative the single outcome r was given our prior knowledge $p(0), p(1)$ of the state, irrespective of the information conveyed by r . Whereas the surprisal $\lambda(r)$ (Eq. 9) specifies the distinguishability of the measurement along with the direction of information gain, $\text{Tr}(\hat{s}_r)$ specifies only how much the measurement distinguished the state in the measurement basis without specifying what was distinguished. In the extreme limit of maximally informative measurement where $p(r|0)$ and $p(r|1)$ limit to delta functions at ± 1 , the surprisal $\lambda(r) \mapsto \pm\infty$ while $\text{Tr}(\hat{s}_r)$ limits to $+\infty$ in both cases, indicating collapse to one of the definite states without specifying which.

For a sequence of measurements, this linear update dramatically simplifies bookkeeping [8, 9, 31]; for example,

$$\hat{s}_{r_1, r_2} \equiv (\hat{L}_{r_2} \hat{L}_{r_1}) \hat{\rho} (\hat{L}_{r_2} \hat{L}_{r_1})^\dagger, \quad p(r_1, r_2) = \bar{p}(r_1) \bar{p}(r_2) \text{Tr}(\hat{s}_{r_1, r_2}). \quad (13)$$

For measurements in other bases, the measurement operators in Eqs. (9) and (10) generalize to

$$\hat{M}_r = \exp \left[\left(\alpha_0(r) \hat{1} + \sum_{k=1}^3 \alpha_k(r) \hat{\sigma}_k \right) / 2 \right], \quad \hat{L}_r = \exp \left[\sum_{k=1}^3 \alpha_k(r) \hat{\sigma}_k / 2 \right], \quad (14)$$

where $\alpha_\mu(r) \in \mathbb{R}$ for $\mu = 0, 1, 2, 3$, which directly parallels Eq. (4) for unitary evolution. Analogously to the global phase ϕ_0 in the unitary case, $\alpha_0(r) = \ln \bar{p}(r)$ contributes only to the scaling of the state before normalization, so is omitted for the minimal operator \hat{L}_r .

The two types of transformations, unitary in Eq. (4) and measurement in Eqs. (10) and (14), have fundamentally different geometric properties that will prove central to the correspondence developed in the next section. For example, unitary evolution generated by $\hat{\sigma}_z$ is elliptic,

$$e^{-i\hat{\sigma}_z\phi/2} = \hat{1} \cos(\phi/2) - i\hat{\sigma}_z \sin(\phi/2), \quad (15)$$

while backaction generated by measuring $\hat{\sigma}_z$ is hyperbolic,

$$e^{\hat{\sigma}_z\alpha/2} = \hat{1} \cosh(\alpha/2) + \hat{\sigma}_z \sinh(\alpha/2). \quad (16)$$

Notably, hyperbolic transformations yield asymptotic fixed points, unlike elliptic transformations. That is, if one were to obtain the same measurement outcome r with the same strength $\alpha(r)$ repeatedly, then the state would converge to a fixed measurement eigenstate. For example, $\alpha(r) > 0$ would yield,

$$\lim_{n \rightarrow \infty} \frac{\hat{L}_r^n |\psi\rangle}{\|\hat{L}_r^n |\psi\rangle\|} = \lim_{n \rightarrow \infty} \frac{e^{n\hat{\sigma}_z\alpha(r)/2}}{\sqrt{p(0)e^{n\alpha(r)} + p(1)e^{-n\alpha(r)}}} |\psi\rangle = \lim_{n \rightarrow \infty} (|0\rangle\langle 0| + e^{-n\alpha(r)} |1\rangle\langle 1|) \frac{|\psi\rangle}{\sqrt{p(0)}} = |0\rangle, \quad (17)$$

while $\alpha(r) < 0$ would yield the fixed point $|1\rangle$. In stark contrast, repeated unitary rotations are periodic and never converge to a fixed point.

In addition to the informational backaction \hat{L}_r , measurement can also include non-informational backaction in the form of conditioned unitary dynamics \hat{U}_r , yielding a composite transformation,

$$\hat{R}_r \equiv \hat{U}_r \hat{L}_r, \quad |\tilde{\psi}_r\rangle \equiv \hat{R}_r |\psi\rangle, \quad \hat{s}_r \equiv \hat{R}_r \hat{\rho} \hat{R}_r^\dagger, \quad (18)$$

with the same probability as in Eq. (11). This general form for an efficient measurement operator thus has an exponential representation weighting the Pauli operators with complex parameters,

$$\hat{R}_r = \exp \left(\sum_{k=1}^3 \zeta_k(r) \hat{\sigma}_k / 2 \right), \quad \zeta_k(r) \equiv \alpha_k(r) - i\phi_k(r) \in \mathbb{C}, \quad (19)$$

and is thus an element of the closed special linear group $\text{SL}(2, \mathbb{C})$.

Sequences of measurements yield quantum state trajectories [1–16] that depend on the entire history (r_1, \dots, r_n) of measurement results,

$$|\tilde{\psi}_{r_1, r_2, \dots, r_n}\rangle = \hat{R}_{r_n} \cdots \hat{R}_{r_2} \hat{R}_{r_1} |\psi\rangle, \quad \hat{s}_{r_1, r_2, \dots, r_n} = (\hat{R}_{r_n} \cdots \hat{R}_{r_2} \hat{R}_{r_1}) \hat{\rho} (\hat{R}_{r_n} \cdots \hat{R}_{r_2} \hat{R}_{r_1})^\dagger, \quad (20)$$

with corresponding trajectory probabilities,

$$p(r_1, r_2, \dots, r_n) = [\bar{p}(r_1) \bar{p}(r_2) \cdots \bar{p}(r_n)] \langle \tilde{\psi}_{r_1, r_2, \dots, r_n} | \tilde{\psi}_{r_1, r_2, \dots, r_n} \rangle, \quad (21a)$$

$$p(r_1, r_2, \dots, r_n) = [\bar{p}(r_1) \bar{p}(r_2) \cdots \bar{p}(r_n)] \text{Tr}(\hat{s}_{r_1, r_2, \dots, r_n}). \quad (21b)$$

A continuous-time formulation of such a quantum state trajectory can be formally obtained by interpreting the complex $\zeta_k(r)$ weighting the generators $\hat{\sigma}_k$ as integrations over the time interval Δt between each measurement, $\zeta_k(r) = \int_0^{\Delta t} [\gamma_k(t) - i\omega_k(t)] dt$, with the observed stochastic results $\zeta_k(r)$ interpreted as averages over Δt of finer-grained stochastic rates $\gamma_k(t)$ and $\omega_k(t)$. When this formal interpolation is possible, the state trajectory is effectively generated by a stochastic non-Hermitian time-dependent Hamiltonian $\hat{R}_r = \exp(-i \int_0^{\Delta t} \hat{H}_{\text{eff}}(t) dt / \hbar)$ with $\hat{H}_{\text{eff}}(t) = \sum_k \hbar(\omega_k(t) + i\gamma_k(t)) \hat{\sigma}_k / 2$. Notably, deterministic non-Hermitian Hamiltonians are a special case of this sort of continuous-time interpolation.

We focus on a Gaussian measurement as a key example of a stochastic qubit state trajectory that admits a continuous-time interpolation [94], where the result r for each interval Δt is sampled from conditional Gaussian distributions centered at distinct means $\pm \bar{r}$ for each measured qubit state,

$$p(r|0) = \sqrt{\frac{\Gamma \Delta t}{\pi}} \exp\left(-\Gamma \Delta t(r - \bar{r})^2\right), \quad p(r|1) = \sqrt{\frac{\Gamma \Delta t}{\pi}} \exp\left(-\Gamma \Delta t(r + \bar{r})^2\right). \quad (22)$$

Since the variance of each distribution, $1/(2\Gamma \Delta t)$, inversely depends on the time interval Δt , the average $\bar{r} = \sum_{k=1}^n r_k/n$ of a sequence of stochastic results (r_1, \dots, r_n) will also be Gaussian-distributed with a variance $1/(2\Gamma n \Delta t)$ that inversely depends on the total time interval $n \Delta t$. This variance scaling permits an interpolation to a continuum limit, where each discrete r observed over a finite Δt corresponds to a formal integral over a white-noise process characterized by the single rate parameter Γ . This scaling also further clarifies interpretation of $\text{Tr}(\hat{s}_r)$ in Eq. 12: a sequence of n weaker measurements with strength Γ integrates to a single, stronger measurement with strength $n\Gamma$, which is consistent with calculation of the unnormalized state norm due to a sequence of n measurements:

$$\text{Tr}(\hat{s}_{(r_1, \dots, r_n)}) = e^{\sum_{k=1}^n \lambda(r_k)} p(0) + e^{-\sum_{k=1}^n \lambda(r_k)} p(1) = e^{\bar{\lambda}(\bar{r})} p(0) + e^{-\bar{\lambda}(\bar{r})} p(1), \quad (23)$$

where $\bar{\lambda}$ is the modified surprisal given the conditional Gaussian distributions modified with $\Gamma \Delta t \rightarrow \Gamma(n \Delta t)$ and \bar{r} is the sequence average defined previously. Thus, we may understand the limit of infinitely strong measurement where $\lambda(r) \rightarrow \pm\infty$ as the integration of an infinite sequence of finite strength measurements, in which $\lim_{n \rightarrow \infty} \text{Tr}(\hat{s}_{(r_1, \dots, r_n)}) = +\infty$ coincides with perfect collapse to a measurement eigenstate.

When $\pm \bar{r} = \pm 1$, the observed result r is scaled to the eigenvalues of the monitored observable $\hat{\sigma}_z$, in which case the parameter Γ represents the *measurement-dephasing rate* observed for the ensemble-averaged dynamics,

$$\hat{\rho}(t + \Delta t) = \int \hat{M}_r \hat{\rho} \hat{M}_r^\dagger dr = \frac{1}{2} \left(\hat{1} + e^{-\Gamma \Delta t} [S_x(t) \hat{\sigma}_x + S_y(t) \hat{\sigma}_y] + S_z(t) \hat{\sigma}_z \right). \quad (24)$$

Importantly, as will be discussed further in Section 6, a fixed measurement-dephasing rate Γ is also compatible with a wider class of Gaussian measurements that include both non-unitary collapse backaction and unitary phase-jitter backaction. The ensemble-average dephasing rates from each type of backaction sum in a complementary way to yield the total dephasing rate Γ . Choosing an angle-dependent scaling $\bar{r}(\theta) = \cos \theta$ for the qubit-state-dependent means $\pm \bar{r}(\theta)$ yields such a Gaussian measurement operator with complementary contributions jointly satisfying Eq. (24),

$$\hat{M}_{r,\theta} = \sqrt{\bar{p}(r, \theta)} \hat{U}_{r,\theta} \hat{L}_{r,\theta}, \quad \bar{p}(r, \theta) = \sqrt{\frac{\Gamma \Delta t}{\pi}} \exp\left(-\Gamma \Delta t(r^2 + \cos^2 \theta)\right), \quad (25a)$$

$$\hat{U}_{r,\theta} = \exp(-i\Gamma \Delta t r \sin \theta \hat{\sigma}_z), \quad \hat{L}_{r,\theta} = \exp(\Gamma \Delta t r \cos \theta \hat{\sigma}_z). \quad (25b)$$

The contribution $\hat{L}_{r,\theta}$ represents the informational measurement collapse backaction, while the contribution $\hat{U}_{r,\theta}$ represents the complementary non-informational unitary phase-jitter backaction. Section 6 will clarify that the parameter θ physically corresponds to the choice of detector basis that is measured long after the detector interacts with the qubit: the interaction fixes the ensemble dephasing rate Γ for the qubit but does not pre-determine the post-interaction detector-basis choice corresponding to θ . After rescaling by the $\sqrt{\Delta t}$ -dependent geometric mean probability $\bar{p}(r, \theta)$, the composite transformation has the exponential form of Eq. (19),

$$\hat{R}_{r,\theta} = \frac{\hat{M}_{r,\theta}}{\sqrt{\bar{p}(r, \theta)}} = \hat{U}_{r,\theta} \hat{L}_{r,\theta} = \exp\left(\Gamma \Delta t r e^{-i\theta} \hat{\sigma}_z\right) = \exp(\zeta(r, \theta) \hat{\sigma}_z/2) \in \text{SL}(2, \mathbb{C}), \quad (26)$$

in terms of a complex angle $\zeta(r, \theta) = 2\Gamma \Delta t r e^{-i\theta}$ that is linear in $\Delta t r$ [63]. The continuum limit to a white noise process can then be taken, formally yielding for each infinitesimal time step dt an observed signal $\Delta t r \rightarrow dt r = dt \cos \theta \text{Tr}(\hat{\sigma}_z \hat{\rho}(t)) + dW/\sqrt{2\Gamma}$ that approximately tracks the mean of $\cos \theta \hat{\sigma}_z$ in the state $\hat{\rho}(t)$ with additive zero-mean white noise described by a stochastic Wiener increment dW with variance dt . Expanding the normalized state update $\hat{\rho}(t + dt) = \hat{R}_{r,\theta} \hat{\rho}(t) \hat{R}_{r,\theta}^\dagger / \text{Tr}[\hat{R}_{r,\theta}^\dagger \hat{R}_{r,\theta} \hat{\rho}(t)]$ to linear order in dt using the Itô rule $dW^2 = dt$ then yields the Itô picture (forward-difference) stochastic differential equation,

$$d\hat{\rho}(t) = \frac{\Gamma}{2} (\hat{\sigma}_z \hat{\rho}(t) \hat{\sigma}_z - \hat{\rho}(t)) dt + \sqrt{2\Gamma} \left(\frac{e^{-i\theta} \hat{\sigma}_z \hat{\rho}(t) + e^{i\theta} \hat{\rho}(t) \hat{\sigma}_z}{2} - \cos \theta \text{Tr}(\hat{\sigma}_z \hat{\rho}(t)) \hat{\rho}(t) \right) dW, \quad (27)$$

with the θ -independent ensemble-averaged dynamics in the expected form of a Lindblad master equation ($dW \rightarrow 0$), modified by a θ -dependent innovation term linear in the zero-mean additive white noise dW .

3 Kinematical Correspondence

The group $\text{SL}(2, \mathbb{C})$ appearing in Eq. (19) is the spinor representation of the (proper orthochronous) Lorentz group $\text{SO}^+(1, 3)$ [70] and establishes a direct correspondence between spacetime structure and qubit transformations. That is, unitary Hamiltonian evolution has the same mathematical structure as a spatial rotation, while the measurement of a detector result r has the same mathematical structure as a Lorentz boost (after factoring out the mean probability $\bar{p}(r)$ from the transformation of the unnormalized state \hat{s}_r).

To emphasize this point, consider the simple example of a spacetime particle with rest-mass m and four-momentum \underline{p} . Starting the particle initially at rest, a Lorentz boost yields,

$$\underline{p} = (mc, \vec{0}) \quad \rightarrow \quad \underline{p}' = (\gamma mc, \gamma mc \vec{\beta}), \quad (28)$$

where $\vec{\beta} = \vec{v}/c = (v_1, v_2, v_3)/c$ is the resulting velocity fraction after the boost and $\gamma = 1/\sqrt{1 - |\vec{\beta}|^2}$ is the Lorentz time-dilation factor. The basis of unit vectors for the four-momentum \underline{p} can then be represented using the four Pauli matrices $(\hat{1}, \hat{\sigma}_1, \hat{\sigma}_2, \hat{\sigma}_3)$, after which the Lorentz transformation has a double-sided matrix representation,

$$\hat{p} = mc\hat{1} \quad \rightarrow \quad \hat{p}' = \hat{L}\hat{p}\hat{L}^\dagger = \gamma mc\hat{1} + \gamma mc \sum_{k=1}^3 \beta_k \hat{\sigma}_k \quad (29)$$

involving the boost (spinor) matrix

$$\hat{L} = \exp(\alpha \hat{v}/2) = \cosh(\alpha/2)\hat{1} + \sinh(\alpha/2)\hat{v}, \quad \tanh \alpha = |\vec{\beta}|, \quad \hat{v} = \sum_{k=1}^3 \frac{v_k}{|\vec{v}|} \hat{\sigma}_k \quad (30)$$

that depends on the hyperbolic rapidity angle α and the matrix representation of the velocity unit vector direction \hat{v} . Using this matrix representation, the four-momentum \hat{p} has the same structure as the unnormalized qubit density matrix \hat{s} in Eq. (10), while the boost transformation has the same structure as the qubit measurement in Eq. (14).

More generally, a Lorentz transformation matrix $\hat{R} = \hat{U}\hat{L} \in \text{SL}(2, \mathbb{C})$ composed of both a unitary spatial rotation \hat{U} and boost \hat{L} is a two-sided (spinor) representation of a Lorentz transformation analogous to Eq. (18). This equivalence arises because $\text{SL}(2, \mathbb{C})$ is the double cover of the (proper orthochronous) Lorentz group $\text{SO}^+(1, 3)$, in the same way that the sub-group of unitary qubit transformations $\text{SU}(2, \mathbb{R}) \subset \text{SL}(2, \mathbb{C})$ is a double cover of the orthogonal group $\text{SO}(3) \subset \text{SO}^+(1, 3)$ of spatial rotations. This representation of

four-vectors and their Lorentz transformations has been long studied in the context of spin groups [66, 67, 70] and Clifford algebras [69, 72].

Pragmatically, this means that the 3-dimensional Bloch vector representation \vec{S} (with transformations in $\text{SO}(3)$) of a normalized qubit state $\hat{\rho}$ (with transformations in $\text{SU}(2, \mathbb{R})$) can be directly generalized to a 4-dimensional vector in spacetime (with transformations in $\text{SO}^+(1, 3)$) that represents an unnormalized qubit state \hat{s} (with transformations in $\text{SL}(2, \mathbb{C})$). Conversely, a relativistic four-vector like the four-momentum \underline{p} of a point particle can be represented as a matrix \hat{p} analogous to an unnormalized qubit density matrix \hat{s} ,

$$\hat{p} = \frac{E}{c} \hat{1} + p_x \hat{\sigma}_x + p_y \hat{\sigma}_y + p_z \hat{\sigma}_z = p^\mu \hat{\sigma}_\mu = p_\mu \hat{\sigma}^\mu, \quad \hat{s} = s^\mu \hat{\sigma}_\mu = s_\mu \hat{\sigma}^\mu, \quad (31)$$

where for convenience we introduce contravariant (raised-index) components p^μ matched with the (lowered-index) Pauli basis $\hat{\sigma}_\mu$ and covariant (lowered-index) components $p_\mu = \eta_{\mu\nu} p^\nu$ matched with the (raised-index) reciprocal Pauli basis $\hat{\sigma}^\mu = \eta^{\mu\nu} \hat{\sigma}_\nu$, as well as the implied summation convention for matched pairs of raised and lowered Greek spacetime indices $\mu = 0, 1, 2, 3$. We use the spacetime metric $\eta_{\mu\nu}$ with signature $(+, -, -, -)$ and nonzero components $\eta_{00} = \eta^{00} = 1$ and $\eta_{kk} = \eta^{kk} = -1$ for $k = 1, 2, 3$.

The Minkowski inner product between four-vectors takes the matrix form

$$\langle \hat{a}, \hat{b} \rangle = \frac{1}{2} \text{Tr}(\tilde{\hat{a}} \hat{b}) = a_0 b_0 - \vec{a} \cdot \vec{b} = a^\mu b_\mu, \quad \langle \hat{\sigma}_\mu, \hat{\sigma}_\nu \rangle = \eta_{\mu\nu}, \quad (32)$$

where the tilde denotes the Clifford conjugate for the Pauli algebra that transposes products, $\widehat{\hat{A}\hat{B}} = \tilde{\hat{B}}\tilde{\hat{A}}$, and changes the Pauli basis to the reciprocal basis, e.g. $\tilde{\hat{p}} = p_0 \hat{1} - p_i \hat{\sigma}_i$ [66, 71, 72]. The inner product is invariant under common Lorentz transformations, $\hat{a} \mapsto \hat{R}\hat{a}\hat{R}^\dagger$ and $\hat{b} \mapsto \hat{R}\hat{b}\hat{R}^\dagger$, because the conjugate of a Lorentz group element is its inverse, $\tilde{\hat{R}} = \hat{R}^{-1}$.

Notably, the determinant of the matrix \hat{p} evaluates to its squared magnitude,

$$\det \hat{p} = \langle \hat{p}, \hat{p} \rangle = p_0^2 - \vec{p} \cdot \vec{p} = p^\mu p_\mu = (mc)^2, \quad (33)$$

and is invariant under Lorentz transformations since $\det(\hat{R}\hat{p}\hat{R}^\dagger) = \det \hat{R} \det p \det \hat{R}^\dagger = \det \hat{p}$.

The qubit analog of an invariant magnitude,

$$\det \hat{s} = \frac{\text{Tr}(\hat{s})^2 - \text{Tr}(\hat{s}^2)}{2} = \text{Tr}(\hat{s})^2 \frac{1 - \text{Tr}(\hat{\rho}^2)}{2} = s_0^2 S_L(\hat{\rho}), \quad (34)$$

is proportional to the linear entropy $S_L(\hat{\rho}) = 2(1 - \text{Tr}(\hat{\rho}^2))$ satisfying $0 \leq S_L \leq 1$. Unlike $S_L(\hat{\rho})$, $\det \hat{s}$ is invariant under measurement backaction. Similarly generalized definitions of linear entropy have been explored in the study of entropy production in non-Hermitian systems [49]. As such, pure states, which satisfy $\det \hat{s} = 0$, are the qubit analog of massless particles, which satisfy $\det \hat{p} = 0$. Similarly, mixed states, which satisfy $\det \hat{s} > 0$, are the qubit analog of massive particles, which satisfy $\det \hat{p} > 0$. Likewise, we find that the inner product between two unnormalized density matrices

$$\langle \hat{a}, \hat{b} \rangle = a_0 b_0 S_L(\hat{\rho}_A, \hat{\rho}_B) \quad (35)$$

is proportional to the linear cross entropy $S_L(\hat{\rho}_A, \hat{\rho}_B) = 2(1 - \text{Tr}(\hat{\rho}_A \hat{\rho}_B))$ of $\hat{\rho}_A = \hat{a}/\text{Tr} \hat{a}$ and $\hat{\rho}_B = \hat{b}/\text{Tr} \hat{b}$ [95].

The spacetime analog of the normalized density matrix $\hat{\rho} = \hat{s}/\text{Tr}(\hat{s})$ is the velocity fraction

$$\hat{\beta} = \frac{\hat{p}}{\text{Tr} \hat{p}} = \frac{1}{2} \left(\hat{1} + \frac{p_j}{p_0} \hat{\sigma}_j \right) = \frac{1}{2} \left(\hat{1} + \frac{v_j}{c} \hat{\sigma}_j \right) \quad (36)$$

due to the relation

$$\frac{\vec{p}}{p_0} = \frac{\vec{p}c}{E} = \frac{\vec{v}}{c} \quad (37)$$

that holds for both massive and massless particles. In the special case of a massless particle, $\vec{\beta} = \vec{v}/c$ is the unit-vector direction of propagation. Massive particles at rest have a Bloch-like velocity description analogous to a maximally mixed qubit state, while massless particles have a velocity description analogous to pure qubit states,

$$\hat{p} = mc\hat{1} \mapsto \hat{\beta} = \frac{\hat{p}}{\text{Tr } \hat{p}} = \frac{\hat{1}}{2} \quad \hat{p} = \hbar(\omega\hat{1}/c + k_x\hat{\sigma}_x) \mapsto \hat{\beta} = \frac{\hat{p}}{\text{Tr}(\hat{p})} = \frac{1}{2}(\hat{1} + \hat{\sigma}_x) = |x\rangle\langle x|. \quad (38)$$

The particle's spacetime displacement \hat{x} is proportional to the time integral of the velocity fraction $\hat{\beta}$,

$$\hat{x}(t) = 2c \int_0^t ds \hat{\beta}(s) = ct\hat{1} + \sum_{k=1}^3 x_k(t)\hat{\sigma}_k \quad \hat{\phi}(t) = 2 \int_0^t ds \hat{\rho}(s) = t\hat{1} + \sum_{k=1}^3 \int_0^t ds S_k(s)\hat{\sigma}_k, \quad (39)$$

while the cumulative qubit trajectory $\hat{\phi}(t)$ is the qubit analog of particle position and the factor of 2 ensures $\langle \hat{x}/c, \hat{\sigma}_0 \rangle = \langle \hat{\phi}, \hat{\sigma}_0 \rangle = t$. Normalizing yields a Bloch-like description of the mean velocity fraction,

$$\bar{\hat{\beta}}(t) = \hat{x}(t)/\text{Tr } \hat{x}(t) = \frac{1}{t} \int_0^t ds \hat{\beta}(s) \quad \bar{\hat{\rho}}(t) = \hat{\phi}(t)/\text{Tr } \hat{\phi}(t) = \frac{1}{t} \int_0^t ds \hat{\rho}(s), \quad (40)$$

and its qubit analog $\bar{\hat{\rho}}(t)$: the time-averaged qubit state over its history. Fig. 1 depicts the quantities relevant to the kinematical analogy through examples of hyperbolic and rotational motion (introduced in Sec. 2 and further elaborated in Sec. 4), while Table 1 summarizes the formal correspondence between these quantities.

4 Dynamical Correspondence

We now draw a formal correspondence between the deterministic dynamics of a point charge momentum \hat{p} and the deterministic dynamics of an unnormalized qubit state \hat{s} . (For clarity, we delay treatment of stochastic dynamics until Section 5.) Magnetic fields are the generators of spatial rotations as part of the Lorentz force, and correspond to the unitary Hamiltonian evolution of a qubit. Electric fields are the generators of boosts causing linear acceleration as part of the Lorentz force, and correspond to deterministic measurement backaction on a qubit. Such deterministic non-unitary dynamics generated by a non-Hermitian Hamiltonian has been used productively to model conditional dissipation in open qubit systems, such as that obtained by post-selection on particular outcomes of a dissipative interaction with a bath or measurement apparatus [6, 47, 56, 58, 59, 61].

Focusing first on unitary spatial rotations, the evolution for both a point charge momentum \hat{p} and an unnormalized qubit state \hat{s} with a time parameter t is generated by an anti-Hermitian operator $-i\hat{H} = i\mu\hat{B}$ with units of energy and components that we parameterize with an effective magnetic field $\hat{B} = \sum_{k=1}^3 B_k\hat{\sigma}_k$ up to a scaling factor μ ,

$$\hat{p}(t + dt) = e^{i\mu dt \hat{B}/\hbar} \hat{p}(t) e^{-i\mu dt \hat{B}/\hbar} \quad \hat{s}(t + dt) = e^{-idt \hat{H}/\hbar} \hat{s}(t) e^{idt \hat{H}/\hbar}. \quad (41)$$

We formally include a factor of \hbar to make the exponents properly dimensionless in both cases, and to follow quantum mechanical convention. Expanding to first order in dt yields corresponding von Neumann differential equations that are well-known from Schrödinger-picture quantum dynamics,

$$\frac{d\hat{p}}{dt} = \frac{i\mu}{\hbar} [\hat{B}, \hat{p}] \quad \frac{d\hat{s}}{dt} = -\frac{i}{\hbar} [\hat{H}, \hat{s}], \quad (42)$$

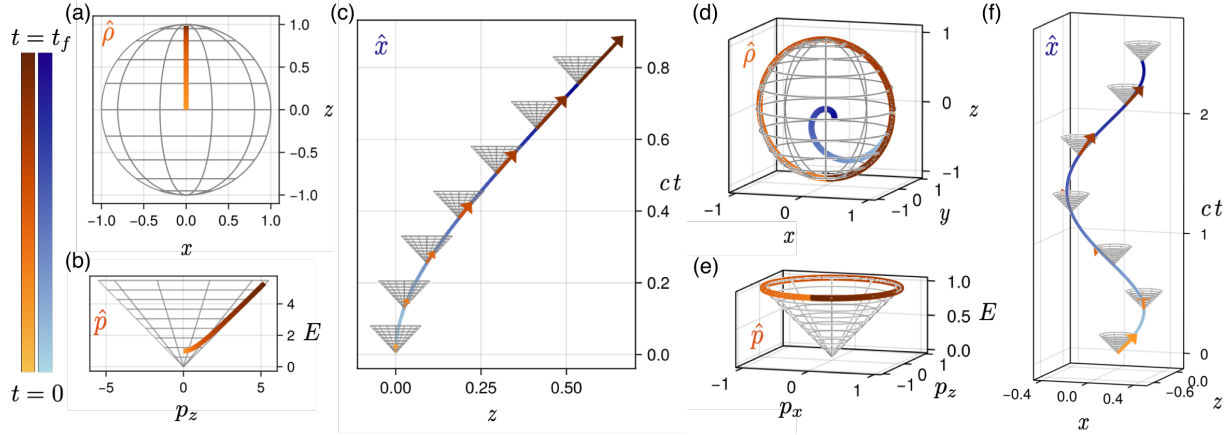


Fig. 1: Visualization of the correspondence between the structure of a qubit and a relativistic point particle for (a-c) hyperbolic purification of a maximally mixed state (corresponding to a massive particle at rest) and (d-f) rotational motion of a pure state $|+x\rangle$ (corresponding to a massless particle moving in the x direction). Time evolution is represented in color going from light to dark. (a) The qubit state $\hat{\rho}$ (point particle velocity $\hat{\beta}$) is purified in the z direction by measurement and asymptotically approaches a pure state (the speed of light). (b) The unnormalized qubit state \hat{s} (particle momentum \hat{p}) is boosted in the z direction, causing the momentum p_z to asymptotically approach the surface of the lightcone. (c) The integrated velocity traces out a relativistic worldline \hat{x} (cumulative state $\hat{\phi}$) in which the particle's lightcone is tangent at each point. (d) The pure qubit state $\hat{\rho}$ (particle velocity $\hat{\beta}$) undergoes Rabi oscillations about $\hat{\sigma}_y$. (e) The unnormalized qubit state \hat{s} corresponds to a particle with momentum \hat{p} initially in the x direction, accelerated around the y axis. (f) The integrated velocity traces out a helical worldline \hat{x} (cumulative state $\hat{\phi}$), which normalizes to the mean velocity $\bar{\beta}$ (time averaged state $\bar{\rho}$) in panel (d).

where $[\hat{A}, \hat{B}] = \hat{A}\hat{B} - \hat{B}\hat{A}$ is a commutator. Expressing these equations in familiar 3-vector notation using Eq. (31) and choosing $\mu = \mu_B(mc/p_0) = (e\hbar/2m)(mc/p_0) = e\hbar c/2p_0$ to be the relativistic generalization of the Bohr magneton (recalling that $\vec{p}/p_0 = \vec{v}/c$), yields

$$c \frac{dp_0}{dt} = W_B = 0, \quad \frac{d\vec{p}}{dt} = \vec{F}_B = e\vec{v} \times \vec{B} \quad \frac{ds_0}{dt} = 0, \quad \frac{d\vec{s}}{dt} = \frac{2\mu_B}{\hbar} \vec{s} \times \vec{B}. \quad (43)$$

We thus recover the expected expressions of magnetic work W_B and magnetic force \vec{F}_B for a massive point charge. Notably, since $mc/p_0 = d\tau/dt$, where τ is the proper time for a massive point particle, the scaled Bohr magneton $\mu = \mu_B d\tau/dt$ is actually momentum-independent and implicitly changes coordinates back to the proper time τ inside the exponent of the transformation in Eq. (41) as a distinguished parameterization for the particle path. For a massless charge with momentum $\underline{p} = (p_0, \vec{p}) = (\hbar\omega/c, \hbar\vec{k})$ such that $|\vec{k}| = \omega/c$, there is no distinguished rest frame with proper time parameter τ , but the choice $\mu = e\hbar c/2p_0 = ec^2/2\omega$ will still remain correctly matched to the time parameter t on a change of frame and yield the same equation $d\vec{p}/dt = e\vec{v} \times \vec{B}$ with $\vec{p}/p_0 = \vec{v}/c = \vec{\beta}$ and $|\vec{\beta}| = 1$. Similarly, after restricting to the non-relativistic (rest frame) Bohr magneton $\mu = \mu_B$, we also recover the expected non-relativistic spin-1/2 Hamiltonian $\hat{H} = -\mu_B \sum_{k=1}^3 B_k \hat{\sigma}_k$ for the energy of a magnetic dipole as well as the expected spin-1/2 state precession dynamics from an external magnetic field.

The probability preserving property $ds_0/dt = 0$ of Hamiltonian evolution for a qubit is analogous to energy conservation $dp_0/dt = 0$ for a point charge due to the fact that magnetic fields do no work. This conservation

Point Particle	Qubit		
Spacetime (Unnormalized) Description			
Four-momentum $\hat{p} = p_0 \hat{1} + \sum_{k=1}^3 p^k \hat{\sigma}_k$	Lorentz transformation $\hat{p} \mapsto \hat{R} \hat{p} \hat{R}^\dagger$	Unnormalized state $\hat{s} = s_0 \hat{1} + \sum_{k=1}^3 s^k \hat{\sigma}_k$	Evolution and measurement $\hat{s} \mapsto \hat{R} \hat{s} \hat{R}^\dagger$
Invariant mass $\det \hat{p} = (mc)^2$	Minkowski inner product $\langle \hat{p}_1, \hat{p}_2 \rangle = E_1 E_2 / c^2 - \vec{p}_1 \cdot \vec{p}_2$	Linear entropy $\det \hat{s} = s_0^2 S_L(\hat{\rho})$	Linear cross entropy $\langle \hat{a}, \hat{b} \rangle = a_0 b_0 S_L(\hat{\rho}_A, \hat{\rho}_B)$
Massless particle $\det \hat{p} = 0$	Propagating along x $\hat{p} = E(\hat{1} + \hat{\sigma}_x)/c$	Pure state $\det \hat{s} = 0$	Polarized along x $\hat{s} = s_0(\hat{1} + \hat{\sigma}_x)$
Massive particle $\det \hat{p} > 0$	At rest $\hat{p} = mc\hat{1}$	Mixed state $\det \hat{s} > 0$	Maximally mixed $\hat{s} = s_0\hat{1}$
Displacement $\hat{x}(t) = 2c \int_0^t ds \hat{\beta}(s)$		Cumulative state $\hat{\phi} = 2 \int_0^t ds \hat{\rho}(s)$	
Bloch Ball (Normalized) Description			
Velocity fraction $\hat{\beta} = \hat{p} / \text{Tr } \hat{p} = [\hat{1} + \sum_{k=1}^3 (v_k/c) \hat{\sigma}_k]/2$		Normalized state $\hat{\rho} = \hat{s} / \text{Tr } \hat{s} = [\hat{1} + \sum_{k=1}^3 S_k \hat{\sigma}_k]/2$	
Massless particle $\text{Tr } \hat{\beta}^2 = 1$	Propagating along x $\hat{\beta} = (\hat{1} + \hat{\sigma}_x)/2$	Pure state $\text{Tr } \hat{\rho}^2 = 1$	Polarized along x $\hat{\rho} = (\hat{1} + \hat{\sigma}_x)/2$
Massive particle $\text{Tr } \hat{\beta}^2 < 1$	Particle at rest $\hat{\beta} = \hat{1}/2$	Mixed state $\text{Tr } \hat{\rho}^2 < 1$	Maximally mixed $\hat{\rho} = \hat{1}/2$
Mean velocity $\bar{\hat{\beta}} = \hat{x} / \text{Tr } \hat{x} = \int_0^t ds \hat{\beta}(s)/t$		Mean state trajectory $\bar{\hat{\rho}} = \hat{\phi} / \text{Tr } \hat{\phi} = \int_0^t ds \hat{\rho}(s)/t$	

Table 1: Summary of the kinematical correspondence between a relativistic point particle (left) and qubit (right). Unnormalized quantities exist in a 4-dimensional spacetime, while normalized quantities exist in a 3-dimensional Bloch ball.

ensures that the dynamics of the corresponding normalized quantities $\hat{\beta} = \hat{p} / \text{Tr } \hat{p}$ and $\hat{\rho} = \hat{s} / \text{Tr } \hat{s}$ have the same von Neumann form,

$$\frac{d\hat{\beta}}{dt} = i\frac{\mu}{\hbar} [\hat{B}, \hat{\beta}] \mapsto \frac{d\vec{v}}{dt} = \vec{a} = \frac{ec}{p_0} \vec{v} \times \vec{B}, \quad \frac{d\hat{\rho}}{dt} = -\frac{i}{\hbar} [\hat{H}, \hat{\rho}] \mapsto \frac{d\vec{S}}{dt} = \frac{2\mu_B}{\hbar} \vec{S} \times \vec{B}, \quad (44)$$

recovering the expected magnetic acceleration \vec{a} of a point charge as well as the expected precession dynamics for the qubit Bloch spin-vector $\vec{S} = \vec{s}/s_0$.

Focusing next on nonunitary boost accelerations, the evolution for both a point charge momentum \hat{p} and an unnormalized qubit state \hat{s} is generated by a Hermitian operator $\hat{D} = \mu \hat{E}/c$ with units of energy and components that we similarly parameterize with an effective electric field $\hat{E} = \sum_{k=1}^3 E_k \hat{\sigma}_k$ up to a scaling

factor μ ,

$$\hat{p}(t+dt) = e^{\mu dt \hat{E}/c\hbar} \hat{p}(t) e^{\mu dt \hat{E}/c\hbar} \quad \hat{s}(t+dt) = e^{dt \hat{D}/\hbar} \hat{s}(t) e^{dt \hat{D}/\hbar}. \quad (45)$$

Expanding to first order in dt yields differential equations,

$$\frac{d\hat{p}}{dt} = \frac{\mu}{\hbar c} \{\hat{E}, \hat{p}\}, \quad \frac{d\hat{s}}{dt} = \frac{1}{\hbar} \{\hat{D}, \hat{s}\}, \quad (46)$$

that involve an anti-commutator $\{\hat{A}, \hat{B}\} = \hat{A}\hat{B} + \hat{B}\hat{A}$ instead of a commutator. Choosing again the relativistic Bohr magneton $\mu = \mu_B(mc/p_0) = e\hbar c/2p_0$ and expanding into 3-vector notation yields,

$$c \frac{dp_0}{dt} = W_E = \vec{v} \cdot (e\vec{E}), \quad \frac{d\vec{p}}{dt} = \vec{F}_E = e\vec{E}, \quad \frac{ds_0}{dt} = \frac{2\mu_B}{\hbar c} \vec{s} \cdot \vec{E}, \quad \frac{d\vec{s}}{dt} = \frac{2\mu_B}{\hbar c} s_0 \vec{E}. \quad (47)$$

We thus recover the expected expressions of electric work W_E and electric force \vec{F}_E for a massive point charge. As with the magnetic case in Eq. (41), the scaling factor $\mu = \mu_B(d\tau/dt)$ implicitly changes coordinates back to the proper time τ inside the exponent of the transformation for the massive case, while for the massless case the factor becomes $\mu = e\hbar c/2p_0 = ec^2/2\omega$ and is explicitly matched with the chosen t parameter to remain invariant under changes of frame. Similarly, choosing the nonrelativistic $\mu = \mu_B$ in the qubit case produces collapse-like dynamics for spin-1/2 generated by an effectively non-Hermitian Hamiltonian $\hat{H}_E = i\hat{D} = i\mu_B \hat{E}/c$.

Electric fields generally do work, so do not conserve energy, $dp_0/dt \neq 0$. Similarly, non-Hermitian qubit dynamics generally do not conserve probability, so $ds_0/dt \neq 0$. This non-conservation induces nonlinear dynamics for the corresponding normalized quantities $\hat{\beta} = \hat{p}/\text{Tr } \hat{p}$ and $\hat{\rho} = \hat{s}/\text{Tr } \hat{s}$,

$$\frac{d\hat{\beta}}{dt} = \frac{\mu}{\hbar c} \{\hat{E}, \hat{\beta}\} - \frac{2\mu}{\hbar c} \text{Tr}(\hat{E}\hat{\beta})\hat{\beta}, \quad \frac{d\hat{\rho}}{dt} = \frac{1}{\hbar} \{\hat{D}, \hat{\rho}\} - \frac{2}{\hbar} \text{Tr}(\hat{D}\hat{\rho})\hat{\rho}. \quad (48)$$

Expanding these equations in 3-vector form using $\mu = e\hbar c/2p_0$ yields,

$$c \frac{d\vec{\beta}}{dt} = \vec{a} = \frac{ec}{p_0} [\vec{E} - (\vec{\beta} \cdot \vec{E})\vec{\beta}], \quad \frac{d\vec{\beta}}{dt} = \frac{2\mu_B}{\hbar c} [\vec{E} - 2(\vec{s} \cdot \vec{E})\vec{s}], \quad (49)$$

which recovers the correct electric acceleration for a point charge, where the role of the nonlinear correction term is to ensure causal propagation with $|\vec{\beta}| \leq 1$. For a normalized qubit state, the corresponding nonlinear correction renormalizes the state to continually reset the total probability back to 1 such that the normalized Bloch vector satisfies $|\vec{s}| \leq 1$.

We now combine the two cases above to consider the action of a full Lorentz transformation involving both spatial rotation and boost acceleration. The corresponding generator $\hat{G} = \hat{D} - i\hat{H} = \mu(\hat{E}/c + i\hat{B}) = \mu\hat{F}$ includes both the Hermitian boost generator \hat{D} and anti-Hermitian rotation generator $-i\hat{H}$ and thus is parameterized by the full electromagnetic field \hat{F} (in Riemann-Silberstein form [73]),

$$\hat{p}(t+dt) = e^{\mu dt \hat{F}/\hbar} \hat{p}(t) e^{\mu dt \hat{F}^\dagger/\hbar}, \quad \hat{s}(t+dt) = e^{dt \hat{G}/\hbar} \hat{s}(t) e^{dt \hat{G}^\dagger/\hbar}. \quad (50)$$

Expanding to first order in dt yields evolution familiar from deterministic non-Hermitian qubit dynamics,

$$\frac{d\hat{p}}{dt} = \frac{2\mu}{\hbar} (\hat{F}\hat{p} + \hat{p}\hat{F}^\dagger) = \frac{2\mu}{\hbar} \{\hat{F}, \hat{p}\}, \quad \frac{d\hat{s}}{dt} = -\frac{i}{\hbar} (\hat{H}_{\text{eff}}\hat{s} - \hat{s}\hat{H}_{\text{eff}}^\dagger) = -\frac{i}{\hbar} [\hat{H}_{\text{eff}}, \hat{s}], \quad (51)$$

in terms of non-Hermitian generalizations of the anti-commutator and commutator,

$$\{\hat{A}, \hat{B}\} = \hat{A}\hat{B} + \hat{B}\hat{A}^\dagger, \quad [\hat{A}, \hat{B}] = \hat{A}\hat{B} - \hat{B}\hat{A}^\dagger, \quad (52)$$

and where $\hat{H}_{\text{eff}} = i\hat{G} = \hat{H} + i\hat{D} = i\mu\hat{F}$ is the effective non-Hermitian Hamiltonian. Expanding Eqs. (51) in 3-vector form using $\mu = e\hbar c/2p_0$ yields the expected work W and Lorentz force \vec{F}_L for a point charge:

$$c \frac{dp_0}{dt} = W = \vec{v} \cdot (e\vec{E}), \quad \frac{d\vec{p}}{dt} = \vec{F}_L = e\vec{E} + e\vec{v} \times \vec{B}, \quad \frac{ds_0}{dt} = \frac{2\mu_B}{\hbar c} \vec{s} \cdot \vec{E}, \quad \frac{d\vec{s}}{dt} = \frac{2\mu_B}{\hbar c} (s_0 \vec{E} + c\vec{s} \times \vec{B}). \quad (53)$$

Similarly, using the non-relativistic $\mu = \mu_B$ in the qubit case produces the spin-1/2 dynamics expected from a general non-Hermitian Hamiltonian.

The corresponding dynamics of the normalized states $\hat{\beta} = \hat{p}/\text{Tr } \hat{p}$ and $\hat{\rho} = \hat{s}/\text{Tr } \hat{s}$ become nonlinear in the state due to the continuous renormalization [8, 46, 48, 60],

$$\frac{d\hat{\beta}}{dt} = \frac{\mu}{\hbar} (\{\hat{F}, \hat{\beta}\} - \text{Tr}[(\hat{F} + \hat{F}^\dagger)\hat{\beta}]\hat{\beta}), \quad \frac{d\hat{\rho}}{dt} = -\frac{i}{\hbar} ([\hat{H}_{\text{eff}}, \hat{\rho}] - \text{Tr}[(\hat{H}_{\text{eff}} - \hat{H}_{\text{eff}}^\dagger)\hat{\rho}]\hat{\rho}). \quad (54)$$

Expanding these equations into 3-vector form using $\mu = e\hbar c/2p_0$ yields,

$$c \frac{d\vec{\beta}}{dt} = \vec{a} = \frac{ec}{p_0} (\vec{E} + \vec{\beta} \times \vec{B} - (\vec{E} \cdot \vec{\beta})\vec{\beta}), \quad \frac{d\vec{S}}{dt} = \frac{2\mu_B}{\hbar c} (\vec{E} + c\vec{S} \times \vec{B} - (\vec{E} \cdot \vec{S})\vec{S}), \quad (55)$$

thus recovering the expected Lorentz acceleration for a point charge. In the qubit case using $\mu = \mu_B$ recovers the expected nonlinear dynamics of the normalized spin-1/2 Bloch vector $|\vec{S}| \leq 1$ under deterministic non-Hermitian dynamics. Note that demanding linearity in $\hat{\beta}$ and $\hat{\rho}$ forces \vec{E} and \hat{D} to vanish and restricts to standard Hermitian quantum theory.

The interplay between hyperbolic and rotational dynamics in electromagnetism provides useful intuition for the analogous non-Hermitian qubit dynamics. Fig. 2(a-c) depicts the simple example of a massless charge in constant electric and magnetic fields—analogously, a pure qubit state undergoing simultaneous hyperbolic and rotational motion. In this example, the electric field $\hat{E} = E_z \hat{\sigma}_z$ and magnetic field $\hat{B} = B_z \hat{\sigma}_z$ commute, paralleling the structure introduced for qubit measurements in Sec. 2. This results in a helical velocity trajectory $\hat{\beta}(t)$ on the Bloch sphere converging towards a fixed point, sweeping out a helical worldline $\hat{x}(t)$ that tightens over time as the particle is accelerated in the z direction and a helical momentum trajectory $\hat{p}(t)$ in the p_x-p_y slice of the lightcone. Notably, the helical path on the Bloch sphere is determined entirely by the angle $\arctan(E_z/cB_z)$ such that $\hat{H}_{\text{eff}} \propto e^{i\arctan(E_z/cB_z)}\hat{\sigma}_z$, which rotates the Hermitian operator $\hat{\sigma}_z$ smoothly into the anti-Hermitian operator $i\hat{\sigma}_z$, offering intuition for the behavior of qubit stochastics on the Bloch sphere that we will elaborate on in Sec. 6.

Interestingly, for the special case of *massless* point charges with $|\vec{\beta}| = 1$, Eqs. (55) can be written in an equivalent form that appears entirely magnetic. That is, using the vector identity $\vec{a} \times (\vec{b} \times \vec{a}) = (\vec{a} \cdot \vec{a})\vec{b} - (\vec{a} \cdot \vec{b})\vec{a}$ and $\vec{\beta} \cdot \vec{\beta} = 1$, Eq. (55) is equivalent to [48]

$$c \frac{d\vec{\beta}}{dt} = \vec{a} = \frac{ec}{p_0} \vec{\beta} \times (\vec{B} + \vec{B}_E), \quad \vec{B}_E = -\vec{\beta} \times \vec{E}, \quad |\vec{\beta}| = 1, \quad (56)$$

which looks like a purely magnetic acceleration from an effective *velocity-dependent* magnetic field \vec{B}_E that emulates the boost effect of the equivalent electric field \vec{E} . The physical reason for this equivalence is that the speed of a massless particle must always be c , so only the direction of the velocity can change. Thus, there always exists an effective magnetic field that can equivalently cause such a change in direction. In contrast to the velocity, the momentum evolution can clearly distinguish boosts from rotations due to the induced changes in energy $E = cp_0$.

Similarly, for the special case of a *pure* qubit state with $|\vec{S}| = 1$, Eqs. (54) can be written in an equivalent form that appears generated by a Hermitian Hamiltonian. That is, for Hermitian \hat{A} and \hat{B} such that $\hat{A}^2 = \hat{A}$

and $\hat{A}\hat{B}\hat{A} = \text{Tr}(\hat{A}\hat{B})\hat{A}$ the commutator identity $[\hat{A}, [\hat{A}, \hat{B}]] = \{\hat{A}^2, \hat{B}\} - 2\hat{A}\hat{B}\hat{A}$ simplifies to $\{\hat{A}, \hat{B}\} - 2\text{Tr}(\hat{A}\hat{B})\hat{A}$, so Eq. (54) is equivalent to

$$\frac{d\hat{\rho}}{dt} = -\frac{i}{\hbar} [\hat{H} + \hat{H}_D, \hat{\rho}], \quad \hat{H}_D = -i[\hat{\rho}, \hat{D}], \quad \hat{\rho}^2 = \hat{\rho}, \quad (57)$$

which looks like purely Hermitian Hamiltonian dynamics from an effective *state-dependent* (i.e., *feedback*) Hamiltonian \hat{H}_D that emulates the collapse-like effects of the equivalent non-Hermitian Hamiltonian $i\hat{D}$. The reason for this equivalence is that a pure state represents maximum certainty and is determined by its orientation relative to other states of maximum certainty, encoded as the direction of its unit Bloch vector \vec{S} . Thus, there always exists a Hermitian Hamiltonian that can equivalently cause such a Bloch vector rotation. In contrast, the evolution for the unnormalized state \hat{s} can clearly distinguish Hermitian from non-Hermitian dynamics due to induced changes to the state normalization s_0 , which will be proportional to the total probability of the observed evolution.

Fig. 2(d-f) displays a second example of simultaneous hyperbolic and rotational dynamics in which the electric field $\hat{E} = E_z\hat{\sigma}_z$ and the magnetic field $\hat{B} = B_x\hat{\sigma}_x$ anti-commute. This gives rise to purely rotational motion with a modulated frequency of revolution around a great circle of the Bloch sphere, sweeping out an elliptical helix in the y - z slice of spacetime and a tilted, elliptical momentum trajectory on its lightcone. As previously alluded to, this pure, normalized state trajectory can be generated either by the non-Hermitian Hamiltonian $\hat{H} + i\hat{D} = \mu_B(-B_x\hat{\sigma}_x + i(E_z/c)\hat{\sigma}_z)$ that includes a deterministic drift towards negative y , or by a time-dependent, Hermitian feedback-control Hamiltonian $\hat{H} + \hat{H}_D(t)$ with $\hat{H}_D(t) = (\mu_B E_z/c) [\hat{\rho}, \hat{\sigma}_z]$ using knowledge of the state to modulate its rate of rotation around the x -axis. However, while the pure normalized state dynamics are equivalently generated by a non-Hermitian or a Hermitian Hamiltonian, which correspond to two very different implementations for a physical qubit, the unnormalized state dynamics distinguish the two cases. While a feedback control Hamiltonian could reproduce the same normalized dynamics as Fig. 2(d), the momentum trajectory generated under this Hamiltonian would be flat due to probability conservation, rather than tilted as in Fig. 2(e), due to the probability non-conservation of non-Hermitian evolution (equivalently, the energy non-conservation of boosts). Thus, the unnormalized state evolution encodes the Hermiticity of the generating Hamiltonian even for pure states, a notable feature that is absent in the normalized state.

Non-Hermitian Hamiltonians of the form $\hat{H}_{\text{eff}} = \mu_B(-B_x\hat{\sigma}_x + i(E_z/c)\hat{\sigma}_z)$ as in Fig. 2(d-f) are considered in the analysis of dissipative qubit dynamics near exceptional points [96], which correspond here to the case $\text{Tr}(\hat{F}^2)/2 = |\vec{E}|^2/c^2 - |\hat{B}|^2 = 0$. More generally, the Lorentz invariants of the electromagnetic field classify the motion of a test charge suspended in the fields, ranging between elliptical motion $\text{Tr}(\hat{F}^2) < 0$ (i.e. PT-symmetric phase of a dissipative qubit), parabolic $\text{Tr}(\hat{F}^2) = 0$ (i.e. exceptional phase), and hyperbolic motion $\text{Tr}(\hat{F}^2) > 0$ (i.e. PT-broken phase).

5 Stochastic Correspondence

The previous section established a formal correspondence between the deterministic Lorentz-force dynamics of a point charge in spacetime and the deterministic dynamics of a qubit subject to a non-Hermitian Hamiltonian. However, as reviewed in Section 2, qubit measurement dynamics are generally stochastic, so should correspond to the dynamics of a point charge subject to stochastic Lorentz forces caused by fluctuating electromagnetic fields. In this section, we examine the dynamical structure of such stochastic Lorentz forces and highlight the peculiar constraints the fluctuating electromagnetic fields must satisfy to fully correspond to stochastic qubit measurement dynamics.

To accommodate stochastic Lorentz transformations, the deterministic generator in Eq. (50) generalizes to a stochastic process, and the dynamical map that advances by this time increment has the same form as

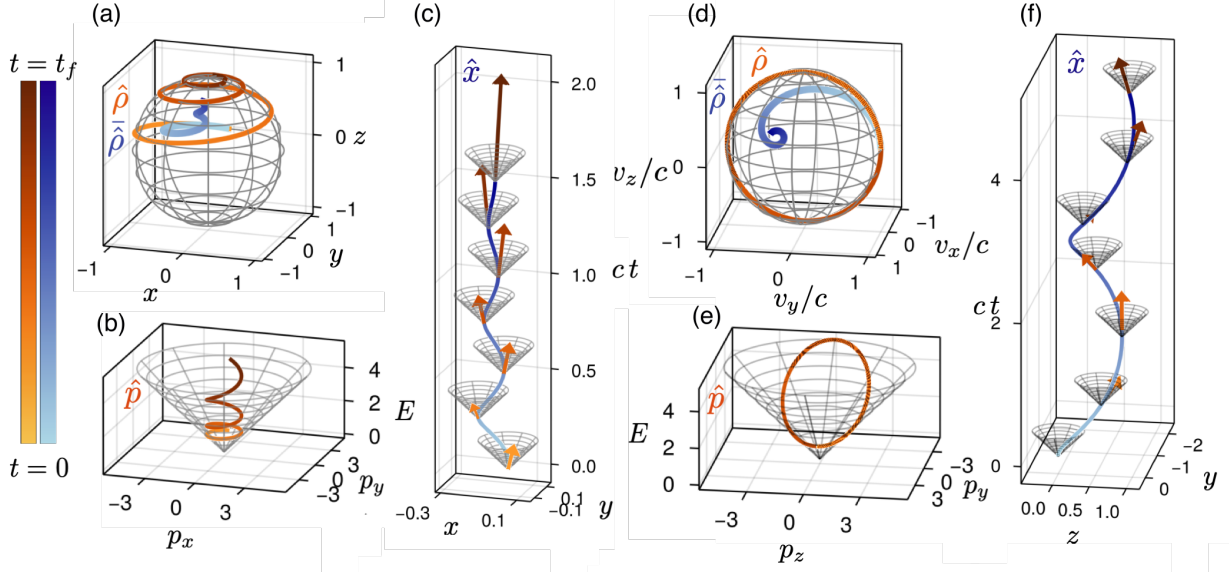


Fig. 2: Combined hyperbolic and rotational motions for a pure qubit state initially in $|+y\rangle$, corresponding to a massless particle with velocity initially moving along $+y$. (a-c) Evolution generated by $\hat{H}_{\text{eff}} = \mu(B_z + iE_z/c)\hat{\sigma}_z$ with $E_z/cB_z = 1/8$. (a) The non-Hermitian boost in $\hat{\sigma}_z$ generates hyperbolic evolution of $\hat{\rho}$ ($\hat{\beta}$) towards the qubit $|0\rangle$ state (z velocity), with simultaneous rotation about $\hat{\sigma}_z$ resulting in spiraling motion that stabilizes at the fixed point $|0\rangle$. (b-c) The helical momentum \hat{p} (unnormalized qubit state \hat{s}) (b) and worldline \hat{x} (c) appear increasingly timelike in the x - y slice of spacetime as the particle is boosted in the z direction, corresponding to the normalized qubit state $\hat{\phi}$ (blue, panel (a)) converging to the fixed point. (d-f) Evolution generated by $\hat{H}_{\text{eff}} = \mu(B_x\hat{\sigma}_x + i(E_z/c)\hat{\sigma}_z)$ with $E_z/cB_x = 2/3$. (d) The non-commutativity of $\hat{\sigma}_x$ and $\hat{\sigma}_z$, with $E_z/cB_x < 1$, gives rise to Bloch sphere rotations with modulated effective frequency, evidenced by the bias of the mean velocity (blue) towards $-y$. (f) Elliptical helix of the worldline, elongated due to the competing electric and magnetic forces.

Eq. (50),

$$\hat{p}(t + dt) = e^{\mu dt \hat{F}/\hbar} \hat{p}(t) e^{\mu dt \hat{F}^\dagger/\hbar} \quad \hat{s}(t + dt) = e^{-i dt \hat{H}_{\text{eff}}/\hbar} \hat{s}(t) e^{i dt \hat{H}_{\text{eff}}^\dagger/\hbar}. \quad (58)$$

This group structure is thus independent of the specifics of the fluctuations that are implicit to $dt\hat{F}$.

Anticipating a correspondence to the diffusive qubit measurement in Eq. (27), we focus on fluctuations that can be approximated by additive zero-mean white noise. In this case, the stochastic generator

$$\hat{F} = \hat{F}_D + \hat{F}_\xi, \quad \hat{H}_{\text{eff}} = \hat{H}_D + \hat{H}_\xi \quad (59)$$

can be separated into deterministic generators of the mean dynamics $\mu dt \hat{F}_D = -idt \hat{H}_D$ that scale linearly with dt , and fluctuating zero-mean generators $\mu dt \hat{F}_\xi = -idt \hat{H}_\xi$ that scale as \sqrt{dt} such that $(\mu dt \hat{F}_\xi)^2 \propto dt$ and $(-idt \hat{H}_\xi)^2 \propto dt$. The fluctuations $dt \hat{F}_\xi$ may be decomposed into real and imaginary parts $dt \hat{F}_\xi = dt \hat{E}_\xi/c + idt \hat{B}_\xi$ that correspond to the electric and magnetic field components of the fluctuations, which may or may not be correlated. The ensemble covariance properties of the fluctuations are characterized by their quadratic

Point Charge	Qubit
Spacetime (Unnormalized) Dynamics	
Generators of Lorentz Transformations	
Electromagnetic Field $\hat{F} = \hat{E}/c + i\hat{B}$	Effective (Non-Hermitian) Hamiltonian $-i\hat{H}_{\text{eff}} = -i(\hat{H} + i\hat{D})$
Lorentz Transformations	
$\hat{p}(t + dt) = e^{\mu dt \hat{F}/\hbar} \hat{p}(t) e^{\mu dt \hat{F}^\dagger/\hbar}$	$\hat{s}(t + dt) = e^{-idt \hat{H}_{\text{eff}}/\hbar} \hat{s}(t) e^{idt \hat{H}_{\text{eff}}^\dagger/\hbar}$
Lorentz Force $d\hat{p}/dt = \mu\{\hat{F}, \hat{p}\}/\hbar, \quad \mu = \mu_B d\tau/dt$ $\mu_B = (e\hbar)/2m, \quad d\tau/dt = mc/p_0$	von Neumann Equation $d\hat{s}/dt = -i[\hat{H}_{\text{eff}}, \hat{s}]/\hbar$
Bloch Ball (Normalized) Dynamics	
Velocity trajectory $\hat{\beta} = \frac{1}{2} \left(\hat{1} + \sum_{k=1}^3 \beta_k \hat{\sigma}_k \right)$	Qubit trajectory $\hat{p} = \frac{1}{2} \left(\hat{1} + \sum_{k=1}^3 S_k \hat{\sigma}_k \right)$
Velocity ratio $\vec{\beta} = \vec{p}/p_0 = \vec{v}/c$	Bloch vector $\vec{S} = \vec{s}/s_0$
Normalized Lorentz force $d\vec{\beta}/dt = 2\mu \left[\vec{E} + (c\vec{\beta}) \times \vec{B} - (\vec{E} \cdot \vec{\beta}) \vec{\beta} \right] / \hbar$	Normalized von Neumann equation $d\vec{S}/dt = 2 \left[\vec{D} + \vec{S} \times \vec{H} - (\vec{D} \cdot \vec{S}) \vec{S} \right] / \hbar$

Table 2: Summary of the dynamical correspondence between a relativistic point charge (left) and a qubit (right). Unnormalized quantities exist in a 4-dimensional spacetime, while normalized quantities exist in a 3-dimensional Bloch ball. The commutator and anticommutator are defined as $[\hat{A}, \hat{B}] := \hat{A}\hat{B} - \hat{B}\hat{A}^\dagger$ and $\{\hat{A}, \hat{B}\} = \hat{A}\hat{B} + \hat{B}\hat{A}^\dagger$, respectively.

combinations: (i) the (frame-dependent) four-vector to first order in dt ,

$$\begin{aligned}
 (dt\hat{F}_\xi)^\dagger(dt\hat{F}_\xi) &= \left(\frac{dt\vec{E}_\xi \cdot dt\vec{E}_\xi}{c^2} + dt\vec{B}_\xi \cdot dt\vec{B}_\xi \right) \hat{1} + \frac{2i}{c} \sum_{k=1}^3 (dt\vec{E}_\xi \times dt\vec{B}_\xi)_k \hat{\sigma}_k \\
 &= \frac{2dt}{\gamma} \sqrt{\frac{\mu_0}{\epsilon_0}} \left(\frac{\mathcal{E}_\xi}{c} \hat{1} + \sum_k \frac{(\vec{S}_\xi)_k}{c^2} \hat{\sigma}_k \right), \tag{60}
 \end{aligned}$$

proportional to an ensemble-averaged energy density \mathcal{E}_ξ and (Poynting-vector) momentum density \vec{S}_ξ/c^2 for the fluctuations, up to a scaling rate γ ; and, (ii) the (frame-independent) complex scalar with real part equal to the fluctuation Lagrangian [73], to first order in dt ,

$$(dt\hat{F}_\xi)^2 = (dt\vec{E}_\xi \cdot dt\vec{E}_\xi/c^2 - dt\vec{B}_\xi \cdot dt\vec{B}_\xi + 2idt\vec{E}_\xi \cdot dt\vec{B}_\xi/c) \hat{1} = \frac{dt}{\gamma} (\rho_\xi e^{i\phi_\xi})^2 \hat{1}, \tag{61}$$

with ensemble-averaged real magnitude ρ_ξ and phase ϕ_ξ , up to the same scaling rate γ . If \hat{F}_ξ arises from a single white noise process, then it takes the canonical form [73],

$$dt\hat{F}_\xi = \hat{\Sigma}dW/\sqrt{\gamma}, \quad \hat{\Sigma} = \rho_\xi \hat{f}_\xi e^{i\phi_\xi}, \quad (62)$$

where $\hat{f}_\xi^2 = \hat{I}$, and $\hat{\Sigma}$ is a standard-deviation operator satisfying

$$\hat{\Sigma}^\dagger \hat{\Sigma}/2 = \sqrt{\frac{\mu_0}{\epsilon_0}} \left(\frac{\mathcal{E}_\xi}{c} \hat{1} + \sum_k \frac{(\vec{S}_\xi)_k}{c^2} \hat{\sigma}_k \right), \quad \hat{\Sigma}^2 = (\rho_\xi e^{i\phi_\xi})^2 \hat{1}. \quad (63)$$

For qubit measurement Eq. (27), informational backaction for the measurement corresponds to a fluctuating electric field. Such a single-component pure electric field fluctuation has covariance proportional to the energy density \mathcal{E}_ξ , and since $\hat{B}_\xi = 0$ for a purely electric field fluctuation, the field carries no Poynting momentum $\vec{S}_\xi \propto \vec{E}_\xi \times \vec{B}_\xi = 0$. This lack of Poynting momentum is notable, since it indicates a preferred frame for the fluctuating electromagnetic field in the point charge correspondence. That is, a different inertial observer would see the same fluctuating field differently after a passive Lorentz frame transformation,

$$\hat{F}_\xi \mapsto \hat{F}'_\xi = \hat{R}\hat{F}_\xi\hat{R}^{-1} = \hat{E}'_\xi/c + i\hat{B}'_\xi, \quad (64)$$

with an apparent magnetic component \hat{B}'_ξ that would yield a non-zero Poynting momentum $\vec{S}'_\xi \propto \vec{E}'_\xi \times \vec{B}'_\xi \neq \vec{0}$. Since an informational measurement process is what breaks the rotational symmetry of a maximally mixed state in the qubit Bloch sphere, it is no surprise that the field fluctuations corresponding to informational measurement in the spacetime generalization have a preferred frame with broken Lorentz symmetry.

Non-informational (unitary) measurement backaction on a qubit corresponds to a fluctuating magnetic field, while more generally, measurement backaction will take the form Eq. (62) for possibly time-dependent ϕ_ξ . Interestingly, electric-magnetic duality phase shifts $\hat{F}_\xi \mapsto \hat{F}_\xi e^{i\theta}$ [73–75] as seen in the qubit measurement of Eq. (27) preserve the energy-momentum density in Eq. (60), but rotate the phase of the complex Lorentz scalar in Eq. (61) and thus change the character of the preferred-frame fluctuations. We explore the nontrivial consequences of such a duality phase shift in the next section. Null fluctuations that satisfy $(dt\hat{F}_\xi)^2 = 0$, such as $dt\hat{F}_\xi = \rho_\xi(\hat{\sigma}_x + i\hat{\sigma}_y)dW/\sqrt{\gamma}$, have degenerate phase and no preferred frame. Notably, fluctuations based on electromagnetic waves, such as semi-classical models of vacuum fluctuations [77–80], are null in character. Since they have no preferred frame, such null fluctuations do not correspond to diffusive qubit measurements of a particular basis as in Eq. (27).

Expanding Eq. (58) to first order in dt yields a stochastic momentum increment, which similarly decomposes into a mean deterministic part and a zero-mean stochastic part,

$$d\hat{p} = d\hat{p}_D + d\hat{p}_\xi \quad (65)$$

with $d\hat{p}_D$ of order dt and $d\hat{p}_\xi$ of order \sqrt{dt} (for details, see the Appendix), such that

$$d\hat{p}_D = \frac{\mu}{\hbar} \left\{ dt\hat{F}_D, \hat{p} \right\} + \frac{\mu^2}{2\hbar^2} \left\{ dt\hat{F}_\xi, \left\{ dt\hat{F}_\xi, \hat{p} \right\} \right\}, \quad d\hat{p}_\xi = \frac{\mu}{\hbar} \{ dt\hat{F}_\xi, \hat{p} \}. \quad (66)$$

The first term in $d\hat{p}_D$ is the same deterministic term seen in Eq. (51). The additional double anti-commutator term is a consequence of the variance of the fluctuations influencing the mean dynamics, and has been called an ‘anti-dephasing’ dissipator in the context of a stochastic extension to non-Hermitian quantum theory [61].

Expanding the normalized velocity increment to linear order in dt similarly yields,

$$d\hat{\beta} = d\hat{\beta}_D + d\hat{\beta}_\xi, \quad (67)$$

where the stochastic contribution (derived in the Appendix),

$$d\hat{\beta}_\xi = \frac{\mu}{\hbar} \left(\left\{ dt\hat{F}_\xi, \hat{\beta} \right\} - \text{Tr} \left((dt\hat{F}_\xi + dt\hat{F}_\xi^\dagger) \hat{\beta} \right) \hat{\beta} \right) \quad (68)$$

coincides with the innovation term of qubit stochastic master equations [11] like Eq. (27). The form of the deterministic normalized increment (derived in the Appendix),

$$\begin{aligned} d\hat{\beta}_D = & \frac{\mu}{\hbar} \left(\left\{ dt\hat{F}'_D, \hat{\beta} \right\} - \text{Tr} \left(((dt\hat{F}'_D) + (dt\hat{F}'_D)^\dagger) \hat{\beta} \right) \hat{\beta} \right) \\ & + \frac{\mu^2}{\hbar^2} \left((dt\hat{F}_\xi) \hat{\beta} (dt\hat{F}_\xi)^\dagger - \text{Tr} \left((dt\hat{F}_\xi)^\dagger (dt\hat{F}_\xi) \hat{\beta} \right) \hat{\beta} \right), \end{aligned} \quad (69)$$

has two modifications from the deterministic case in Eq. (54) that arise from the influence of the fluctuation variance. The first term in Eq. (69) has the same form as Eq. (54), but includes an effective renormalization of the deterministic generator,

$$dt\hat{F}'_D = dt\hat{F}_D - \frac{\mu}{\hbar} \text{Tr} \left((dt\hat{F}_\xi + (dt\hat{F}_\xi)^\dagger) \hat{\beta} \right) dt\hat{F}_\xi. \quad (70)$$

The second term in Eq. (69) is closely related to the Lindblad ensemble-dephasing term familiar from qubit master equations [12] like Eq. (27).

Notably, the quadratic fluctuation corrections to the deterministic increment $dt\hat{\beta}_D$ contain terms that are nonlinear in $\hat{\beta}$ due to the renormalization of $\hat{\beta}$ after each increment. In contrast, the unnormalized momentum increment $dt\hat{p}_D$ remains linear in \hat{p} since the fundamental group transformation is linear. Since the deterministic mean evolution of a normalized qubit state $\hat{\rho}$ (analogous to $\hat{\beta}$) should still be linear in the normalized state $\hat{\rho}$, as seen in Eq. (27), we conclude that qubit measurements must have additional constraints for their corresponding fluctuating fields $dt\hat{F}_\xi$.

The deterministic mean evolution of $\hat{\beta}$ can be nonlinear due to three renormalization terms: the terms $\text{Tr} \left(dt\hat{F}_\xi^\dagger dt\hat{F}_\xi \hat{\beta} \right) \hat{\beta}$ and $\text{Tr} \left((dt\hat{F}'_D + dt\hat{F}'_D^\dagger) \hat{\beta} \right) \hat{\beta}$ in Eq. (69), and the term $\text{Tr} \left((dt\hat{F}_\xi + dt\hat{F}_\xi^\dagger) \hat{\beta} \right) dt\hat{F}_\xi$ in Eq. (70). Additional constraints on the fluctuating fields can make these terms linear in $\hat{\beta}$, as expected for the analogous qubit measurement. Noting that $\text{Tr} \hat{\beta} = 1$, trace terms of the form $\text{Tr}(\hat{A}\hat{\beta})$ will be independent of $\hat{\beta}$ if $\hat{A} \propto \hat{1}$ and independent of $\hat{\beta}$. Assuming this sufficient condition for the first two renormalization terms produces the following constraints on the fluctuating fields:

$$[\hat{E}_\xi, \hat{B}_\xi] = 0 \quad \leftrightarrow \quad \vec{S}_\xi \propto \vec{E}_\xi \times \vec{B}_\xi = 0, \quad (71)$$

$$\hat{E}'_D = c \left(\frac{\hat{F}'_D + \hat{F}'_D^\dagger}{2} \right) = 0 \quad \leftrightarrow \quad dt\vec{E}_D = \frac{2\mu}{\hbar c} (\vec{\beta} \cdot dt\vec{E}_\xi) dt\vec{E}_\xi. \quad (72)$$

To compensate for the nonlinearity caused by the third term, we constrain the total renormalized generator in Eq. (70) to be independent of $\hat{\beta}$. Since its Hermitian part $\hat{E}'_D = 0$ from Eq. (72), this remaining constraint on the anti-Hermitian part yields,

$$\hat{B}'_D = \frac{\hat{F}'_D - \hat{F}'_D^\dagger}{2i} = dt\hat{B}_0 \quad \leftrightarrow \quad dt\vec{B}_D = dt\vec{B}_0 + \frac{2\mu}{\hbar c} (\vec{\beta} \cdot dt\vec{E}_\xi) dt\vec{B}_\xi, \quad (73)$$

for some $\hat{\beta}$ -independent deterministic magnetic generator \vec{B}_0 .

Under these three conditions, the deterministic mean dynamics of $\hat{\beta}$ in Eq. (69) become linear and precisely reduce to the Lindblad form expected from the qubit master Eq. (27),

$$d\hat{\beta}_D = \frac{i\mu dt}{\hbar} [\hat{B}_0, \hat{\beta}] + \frac{\mu^2}{\hbar^2} \left(dt\hat{F}_\xi \hat{\beta} dt\hat{F}_\xi^\dagger - \frac{1}{2} \{ dt\hat{F}_\xi^\dagger dt\hat{F}_\xi, \hat{\beta} \} \right). \quad (74)$$

Expanding these mean dynamics in 3-vector notation yields,

$$d\vec{\beta}_D = \frac{e\mu dt}{p_0} \vec{\beta} \times \vec{B}_0 + \frac{e^2 c^2}{4p_0^2} \left((\vec{\beta} \times dt\vec{E}_\xi/c) \times dt\vec{E}_\xi/c + (\vec{\beta} \times dt\vec{B}_\xi) \times dt\vec{B}_\xi \right), \quad (75)$$

substituting $\mu = e\hbar c/2p_0$. The corresponding mean momentum evolution under the same linearity conditions takes the form,

$$d\hat{p}_D = \frac{i\mu dt}{\hbar} [\hat{B}_0, \hat{p}] + \frac{2\mu^2}{\hbar^2 c} \text{Tr}(\hat{\beta} dt\hat{E}_\xi) \{ dt\hat{F}_\xi, \hat{p} \} + \frac{\mu^2}{2\hbar^2} \{ dt\hat{F}_\xi, \{ dt\hat{F}_\xi, \hat{p} \} \}, \quad (76)$$

or in vector form,

$$\begin{aligned} d\vec{p}_D &= e\vec{v} \times \left(dt\vec{B}_0 + e(\vec{p} \cdot dt\vec{E}_\xi) dt\vec{B}_\xi \right) + \frac{e^2 c}{2p_0} \left(\frac{3}{c^2} (\vec{v} \cdot dt\vec{E}_\xi) dt\vec{E}_\xi + (\vec{v} \cdot dt\vec{B}_\xi) dt\vec{B}_\xi + dt\vec{E}_\xi \times dt\vec{B}_\xi - \vec{v} (dt\vec{B}_\xi)^2 \right) \\ d\vec{p}_0^D &= \frac{e^2}{p_0 c} (\vec{v} \cdot d\vec{E}_\xi)^2 + \frac{e^2}{2p_0} \left((dt\vec{E}_\xi)^2 - \vec{v} \cdot (dt\vec{E}_\xi \times dt\vec{B}_\xi) \right). \end{aligned} \quad (77)$$

Interestingly, the mean momentum dynamics are reminiscent of runaway self-force solutions: the greater the particle's momentum, the faster it is accelerated.

Returning to the meaning of the constraints, the first constraint to achieve linearity in Eq. (71) states that the Poynting momentum of the zero-mean fluctuations vanishes, which is equivalent to choosing the laboratory frame to be the preferred frame of those fluctuations. The second and third constraints of Eqs. (72) and (73) together imply that the stochastic electromagnetic fields must have an unusual *velocity-dependent* form,

$$dt\hat{F} = \frac{1}{c} \left(\frac{2\mu}{\hbar c} \text{Tr}(dt\hat{E}_\xi \hat{\beta}) dt\hat{E}_\xi + dt\hat{E}_\xi \right) + i \left(dt\hat{B}_0 + \frac{2\mu}{\hbar c} \text{Tr}(dt\hat{E}_\xi \hat{\beta}) dt\hat{B}_\xi + dt\hat{B}_\xi \right), \quad (78)$$

or, equivalently,

$$dt\vec{E} = \frac{2\mu}{\hbar c} (dt\vec{E}_\xi \cdot \vec{\beta}) dt\vec{E}_\xi + dt\vec{E}_\xi \quad dt\vec{B} = dt\vec{B}_0 + \frac{2\mu}{\hbar c} (dt\vec{E}_\xi \cdot \vec{\beta}) dt\vec{B}_\xi + dt\vec{B}_\xi. \quad (79)$$

As seen in Eq. (54) for the deterministic case, the fluctuation-independent field \hat{B}_0 must be purely magnetic in character for the velocity evolution $d\hat{\beta}_D$ to be linear in $\hat{\beta}$, meaning that the velocity must not be boosted on average. However, only fluctuations with a velocity-dependent mean of the specific form in Eq. (78) can preserve that linearity by compensating for the mean boost induced by the fluctuations. The need for this compensating term can thus be understood as a stabilization condition to prevent boosts of the mean reference frame of the charge (i.e., the mean $\hat{\beta}$). Moreover, the form of Eq. (78) implies that observing such a fluctuating electromagnetic field would constitute a noisy measurement of a particular velocity component, in complete analogy to how observing the noisy record r for a continuous qubit measurement as in Eq. (27) constitutes a noisy measurement of a particular qubit observable (which we will carefully consider in the next section). It is curious and notable that demanding linearity of the mean evolution of $\hat{\beta}$ is a sufficient condition to establish such a close correspondence to qubit measurement.

Point Charge	Qubit
Stochastic Spacetime (Unnormalized) Dynamics	
$\hat{F} = \hat{F}_D + \hat{F}_\xi$	Stochastic Generators $\hat{H}_{\text{eff}} = \hat{H}_D + \hat{H}_\xi$
$\hat{p}(t+dt) = e^{\mu dt \hat{F}/\hbar} \hat{p}(t) e^{\mu dt \hat{F}^\dagger/\hbar} \approx \hat{p}(t) + d\hat{p}_D + d\hat{p}_\xi$	Stochastic Lorentz Transformation $\hat{s}(t+dt) = e^{-i dt \hat{H}_{\text{eff}}/\hbar} \hat{s}(t) e^{i dt \hat{H}_{\text{eff}}^\dagger/\hbar} \approx \hat{s}(t) + d\hat{s}_D + d\hat{s}_\xi$
Innovation	
$d\hat{p}_\xi = \mu \{dt \hat{F}_\xi, \hat{p}\}/\hbar$	$d\hat{s}_\xi = \{-idt \hat{H}_\xi, \hat{s}\}/\hbar$
Mean Dynamics	
$d\hat{p}_D = \mu dt \{\hat{F}_D, \hat{p}\}/\hbar + \mu^2 \{dt \hat{F}_\xi, \{dt \hat{F}_\xi, \hat{p}\}\}/2\hbar^2$	$d\hat{s}_D = -idt [\hat{H}_D, \hat{s}]/\hbar + \{dt \hat{H}_\xi, \{dt \hat{H}_\xi, \hat{s}\}\}/2\hbar^2$
Stochastic Bloch Ball (Normalized) Dynamics	
Normalized Stochastic Evolution	
$\hat{\beta}(t+dt) = \hat{p}(t+dt)/\text{Tr}(\hat{p}(t+dt)) \approx \hat{\beta}(t) + d\hat{\beta}_D + d\hat{\beta}_\xi$	$\hat{\rho}(t+dt) = \hat{s}(t+dt)/\text{Tr}(\hat{s}(t+dt)) = \hat{\rho}(t) + d\hat{\rho}_D + d\hat{\rho}_\xi$
Innovation	
$d\hat{\beta}_\xi = \mu (\{dt \hat{F}_\xi, \hat{\beta}\} - \text{Tr}(\{dt \hat{F}_\xi, \hat{\beta}\}) \hat{\beta})/\hbar$	$d\hat{\rho}_\xi = \{-idt \hat{H}_\xi, \hat{\rho}\} - \text{Tr}(\{-idt \hat{H}_\xi, \hat{\rho}\}) \hat{\rho}$
Mean Dynamics	
$d\hat{\beta}_D = \mu \left(\{dt \hat{F}'_D, \hat{\beta}\} - \text{Tr}(\{dt \hat{F}'_D, \hat{\beta}\}) \hat{\beta} \right)/\hbar$ $+ \mu^2 \left(dt \hat{F}_\xi \hat{\beta} dt \hat{F}_\xi^\dagger - \text{Tr}(\{dt \hat{F}_\xi \hat{\beta} dt \hat{F}_\xi^\dagger\}) \hat{\beta} \right)/\hbar^2$	$d\hat{\rho}_D = \left(-i[dt \hat{H}'_D, \hat{\rho}] - \text{Tr}(-i[dt \hat{H}'_D, \hat{\rho}]) \hat{\rho} \right)/\hbar$ $+ \left(dt \hat{H}_\xi \hat{\rho} dt \hat{H}_\xi^\dagger - \text{Tr}(dt \hat{H}_\xi \hat{\rho} dt \hat{H}_\xi^\dagger) \hat{\rho} \right)/\hbar^2$
Effective Generator	
$dt \hat{F}'_D = dt \hat{F}_D - \text{Tr}(\mu \{dt \hat{F}_\xi, \hat{\beta}\}/\hbar) dt \hat{F}_\xi$	$dt \hat{H}'_D = dt \hat{H}_D - \text{Tr}(\{-idt \hat{H}_\xi, \hat{\rho}\}/\hbar) d\hat{H}_\xi$

Table 3: Summary of the stochastic correspondence between a relativistic point charge and a qubit, where $dt \hat{F}_\xi$ and $dt \hat{H}_\xi$ are order \sqrt{dt} . Unnormalized quantities exist in a 4-dimensional spacetime, while normalized quantities exist in a 3-dimensional Bloch ball. The commutator and anticommutator are given by $[\hat{A}, \hat{B}] := \hat{A}\hat{B} - \hat{B}\hat{A}^\dagger$ and $\{\hat{A}, \hat{B}\} = \hat{A}\hat{B} + \hat{B}\hat{A}^\dagger$, respectively.

6 Delayed Choice Lorentz Transformations

For concreteness, we now revisit the θ -dependent continuous Gaussian measurement of a qubit with the measurement operator that we previously introduced in Eq. (25),

$$\hat{R}_{r,\theta} = \exp\left(\Gamma \Delta t r e^{-i\theta} \hat{\sigma}_z\right). \quad (80)$$

We explain in more detail how the parameter θ relates to a delayed choice being made in an experimental implementation, then discuss the implications of such a parameter for the analogous point-particle correspondence.

The measurement operator $\hat{R}_{r,\theta}$ is a good description for the typical readout process of a superconducting qubit, such as a transmon or fluxonium, using circuit quantum electrodynamics (cQED) [97]. In such a superconducting circuit setting, the qubit consists of the lowest two energy levels of an anharmonic oscillator (with energy gap $E_1 - E_0 = \hbar\omega_q$) and is coupled to a harmonic microwave readout resonator of bare frequency

ω_r with amplitude \hat{a} (satisfying $[\hat{a}, \hat{a}^\dagger] = \hat{1}$) that is kept strongly detuned from the qubit. Such a dispersive coupling causes the frequency of the resonator to depend on the qubit state, with an effective interaction Hamiltonian $\hat{H}_{\text{int}} = -\hbar\chi\hat{a}^\dagger\hat{a}\hat{\sigma}_z$, where $\pm\chi$ is the dispersive qubit-dependent frequency shift of the resonator. The readout resonator then couples to a transmission line with amplitude decay rate $\kappa/2$, allowing an input microwave tone to reflect off the resonator then be amplified and recorded with a homodyne measurement to produce a stochastic time series (r_0, r_1, r_2, \dots) of digitized readout signals r_k separated by an integration time steps Δt corresponding to the inverse bandwidth of the homodyne detector. Each readout r_k in the time series corresponds to a measurement operator \hat{R}_{r_k, θ_k} , where θ_k corresponds to the quadrature angle of the output microwave tone that was probed by the homodyne measurement to produce the result r_k .

In more detail, pumping the transmission line with a microwave tone $\varepsilon e^{-i\omega_r t}$ at the bare resonance frequency ω_r adiabatically generates two distinct coherent steady states in the resonator with amplitudes $\alpha_{\pm} = -i(2\varepsilon/\kappa)/(1 \mp i(2\chi/\kappa))$, each with the same mean photon number $\bar{n} = |\alpha_{\pm}|^2 = |2\varepsilon/\kappa|^2/(1 + (2\chi/\kappa)^2)$ but differing phase shifts $\arg(\alpha_{\pm}) = -\pi/2 \pm \arctan(2\chi/\kappa)$. The different θ -dependent resonator quadratures $\hat{I}_{\theta} = (\hat{a}e^{-i\theta} + \hat{a}^\dagger e^{i\theta})/\sqrt{2}$ will thus have varying information about the qubit state. One extreme case is $\hat{I}_0 = (\hat{a} + \hat{a}^\dagger)/\sqrt{2}$, which will have two distinct steady-state means $\text{Re}(\alpha_{\pm}) = \pm\bar{n}(\chi/\varepsilon)$ and thus reveals maximum information about the qubit state. The other extreme case is $\hat{I}_{\pi/2} = -i(\hat{a} - \hat{a}^\dagger)/\sqrt{2}$, which only has a single steady-state mean $\text{Im}(\alpha_{\pm}) = -\bar{n}(\kappa/2\varepsilon)$ and thus reveals no information about the qubit state. Since the resonator state leaks into the transmission line and is later measured, we thus expect distinct types of measurement backaction on the qubit that depend on the measured quadrature angle θ .

The qubit and resonator cannot know what quadrature will be measured in the transmission line at a later time after it propagates to the homodyne detector. This no-signaling constraint forces the ensemble-average dynamics to be θ -independent. To see this formally, note that over a duration Δt each coherent state of the resonator leaks into the transmission line with probability $\kappa\Delta t$, yielding an entangled steady state [15] (where we order the states as $|\text{qubit}\rangle|\text{resonator}\rangle|\text{transmission line}\rangle$ and work in a rotating frame that cancels the additional state-dependent phase evolution from the drive),

$$|\Psi\rangle = c_0 |0\rangle |\alpha_+\rangle \left| \sqrt{\kappa\Delta t} \alpha_+ \right\rangle + c_1 |1\rangle |\alpha_-\rangle \left| \sqrt{\kappa\Delta t} \alpha_- \right\rangle. \quad (81)$$

The reduced qubit-resonator state after tracing out the leaked field in the transmission line,

$$\hat{\rho}_{\text{qr}} = |c_0|^2 |0\rangle\langle 0| \otimes |\alpha_+\rangle\langle\alpha_+| + |c_1|^2 |1\rangle\langle 1| \otimes |\alpha_-\rangle\langle\alpha_-| + e^{-\Gamma\Delta t} (c_0 c_1^* e^{i\omega_S \Delta t} |0\rangle\langle 1| \otimes |\alpha_+\rangle\langle\alpha_-| + \text{h.c.}), \quad (82)$$

thus exhibits ensemble-averaged dephasing and phase precession,

$$e^{-\Gamma\Delta t + i\omega_S \Delta t} = \left\langle \sqrt{\kappa\Delta t} \alpha_- \left| \sqrt{\kappa\Delta t} \alpha_+ \right\rangle \right\rangle = e^{-\kappa\Delta t |\alpha_- - \alpha_+|^2/2 + i\kappa\Delta t \text{Im}(\alpha_-^* \alpha_+)}, \quad (83)$$

at the *measurement-dephasing rate* and *ac-Stark-shift frequency* (up to the omitted drive-induced phase difference) [12, 13, 15],

$$\Gamma = \kappa \frac{|\alpha_- - \alpha_+|^2}{2} = \frac{2}{\kappa} \frac{(2\chi)^2 \bar{n}}{1 + (2\chi/\kappa)^2}, \quad \omega_S = \kappa \text{Im}(\alpha_-^* \alpha_+) = \frac{4\chi\bar{n}}{1 + (2\chi/\kappa)^2}. \quad (84)$$

This reduced state evolution that traces out the transmission line is equivalent to ensemble-averaging over all results measured later on the transmission line. Thus, any choice of quadrature angle θ that is later measured will produce precisely the same ensemble-averaged evolution for the qubit-resonator state.

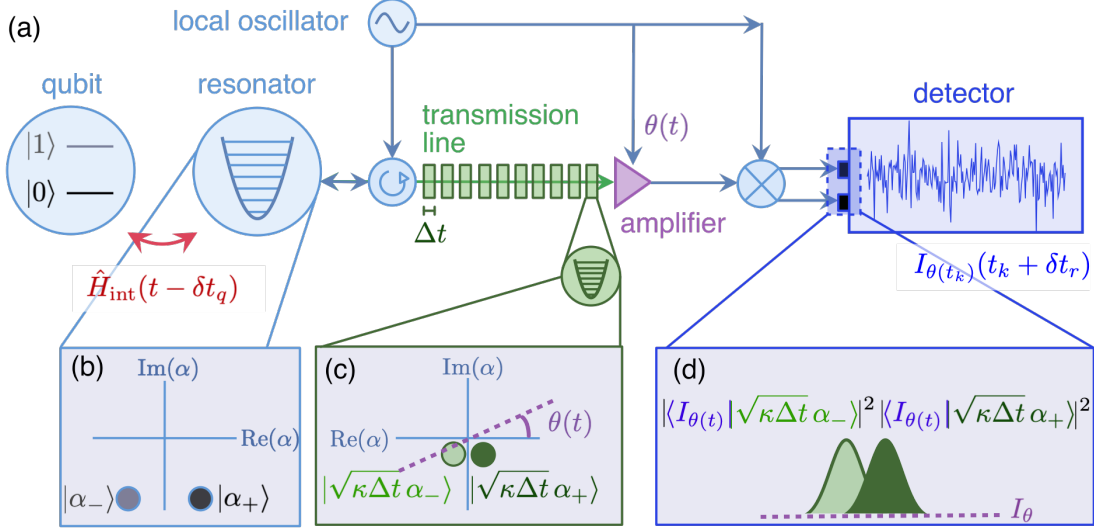


Fig. 3: A superconducting qubit is dispersively coupled to a resonator via $\hat{H}_{\text{int}}(t - \delta t_q)$ (a). This causes the entangled qubit-resonator state to reach a steady-state superposition of $|0\rangle|\alpha_+\rangle$ and $|1\rangle|\alpha_-\rangle$, sketched in (b) as the Husimi-Q function $Q(\alpha)$ of the conditioned resonator states. The resonator is pumped in reflection via the local oscillator, which entangles the qubit-resonator states with traveling transmission line states $|\sqrt{\kappa\Delta t}\alpha_{\pm}\rangle$ discretized by the detector integration time Δt (c). The traveling modes are amplified along a quadrature at angle $\theta(t)$ that can be freely and continuously varied throughout the experiment, which determines whether the qubit undergoes unitary ($\theta = \pi/2$) backaction, non-unitary hyperbolic ($\theta = 0$) backaction, or a combination of both. The mixer multiplies the leaked, amplified resonator field with the LO and low-pass filters the output, yielding a slowly varying homodyne signal $I_{\theta(t)}(t + \delta t_r)$ randomly distributed as a mixture of two real Gaussians due to postselection of the transmission line modes $|\sqrt{\kappa\Delta t}\alpha_{\pm}\rangle$ by the tilted quadrature eigenstate $\langle I_{\theta(t)} |$ (d). This observation at time $t + \delta t_r$ collapses the entangled state, retroactively determining the reduced qubit state at the prior original interaction time $t - \delta t_q$ as a result of the choice of amplification quadrature at time t .

For the actual measurement procedure, shown in Fig. 3, the leaked field propagates down the transmission line unchanged for a time delay δt_q , then at time t passes through a phase-sensitive amplifier that amplifies the quadrature defined by angle $\theta(t)$ and deamplifies the complementary quadrature $\theta(t) + \pi/2$. Equivalently, this can be understood as squeezing the traveling coherent state $|\sqrt{\kappa\Delta t}\alpha_{\pm}\rangle$ along an axis $\theta(t)$ in the complex plane of α_{\pm} . Importantly, the quadrature angle $\theta(t)$ is determined by the relative phase between the amplifier reference pump and the traveling field to be amplified, so can be made long after the traveling field already interacted with the qubit and resonator. The amplified field is then downconverted by mixing with the reference pump and digitized to produce the stochastic homodyne readout $I_{\theta(t)}(t + \delta t_r)$ after another time delay δt_r . The total time delay from the time of interaction to the completion of the readout procedure is $\delta t_q + \delta t_r$, so the measured readout will correspond to (and affect) the *past* state of the qubit and resonator. After a sequence of homodyne measurements $I_{\theta(t_k)}(t_k + \delta t_r)$ have been recorded, the pump is turned off to adiabatically return the readout resonator to the vacuum state, which disentangles the resonator from the qubit to leave a final conditioned qubit state that is entirely determined by the recorded history of measurements.

The collected definite signal $I_{\theta(t)}(t + \delta t_r)$ is proportional to the eigenvalue of the corresponding transmission line quadrature $\hat{I}_{\theta(t)} = (\hat{c}e^{-i\theta(t)} + \hat{c}^\dagger e^{i\theta(t)})/\sqrt{2}$, where \hat{c} is the amplitude of the transmission line mode containing the leaked (and amplified) field. Thus, measuring the result $I_{\theta(t)}(t + \delta t_r)$ at time $t + \delta t_r$ for the quadrature angle θ chosen at time t collapses the entangled state generated by the interaction at time $t - \delta t_q$ in Eq. (81) to leave a conditioned (unnormalized) state of the qubit and resonator:

$$\begin{aligned} \langle \psi_{I_{\theta(t)}(t + \delta t_r)}(t - \delta t_q) \rangle &= c_0 |0\rangle |\alpha_+\rangle \langle I_{\theta(t)}(t + \delta t_r) | \sqrt{\kappa \Delta t} \alpha_+ \rangle + c_1 |1\rangle |\alpha_-\rangle \langle I_{\theta(t)}(t + \delta t_r) | \sqrt{\kappa \Delta t} \alpha_- \rangle \\ &= \left(\hat{M}_{I_{\theta(t)}(t + \delta t_r)} \otimes \hat{1} \right) |\psi(t - \delta t_q)\rangle, \end{aligned} \quad (85)$$

$$\hat{M}_{I_{\theta(t)}(t + \delta t_r)} = \langle I_{\theta(t)}(t + \delta t_r) | \sqrt{\kappa \Delta t} \alpha_+ \rangle |0\rangle \langle 0| + \langle I_{\theta(t)}(t + \delta t_r) | \sqrt{\kappa \Delta t} \alpha_- \rangle |1\rangle \langle 1|, \quad (86)$$

where $|\psi(t - \delta t_q)\rangle = c_0 |0\rangle |\alpha_+\rangle + c_1 |1\rangle |\alpha_-\rangle$ is the joint state of just the qubit and resonator at the time of interaction $t - \delta t_q$, assumed to be adiabatically prepared from the product state $(c_0 |0\rangle + c_1 |1\rangle) |0\rangle$ of a qubit state and the vacuum state of the resonator. The effective measurement operator $\hat{M}_{I_{\theta(t)}(t + \delta t_r)}$ notably affects only the qubit degree of freedom and is diagonal in the $\hat{\sigma}_z$ basis, which is why the intermediate entanglement with the resonator steady states does not impact the final reduced qubit dynamics after adiabatic disentanglement with the resonator at the end of the measurement sequence. This enables the standard Bayesian updates of the form in Eqs. 7, 8, in which efficient quantum measurement appears to maintain purity of a pure qubit state. In fact, the qubit-resonator entanglement causes the reduced qubit state to be mixed during the intervening measurement dynamics. However, the adiabatic assumption forces states of the form $|0\rangle |\alpha_+\rangle$ and $|1\rangle |\alpha_-\rangle$, which can be understood as the true logical states to which Eqs. 7, 8 refer, while adiabatic disentanglement prior to tomography ensures that this subtlety around the definition of the logical states is not important to experimental prediction of the qubit state evolution.

The effective measurement operator in Eq. 85 is determined by the collapse amplitudes from the distinct leaked steady states in the transmission line to the observed homodyne signal $I_{\theta(t)}(t + \delta t_r)$. The probability density for the observed signal $I_{\theta(t)}(t + \delta t_r)$ is correspondingly determined by the Born rule, as anticipated in Eq. (6),

$$p(I_{\theta(t)}(t + \delta t_r)) = \langle \psi(t - \delta t_q) | \left[\hat{M}_{I_{\theta(t)}(t + \delta t_r)}^\dagger \hat{M}_{I_{\theta(t)}(t + \delta t_r)} \otimes \hat{1} \right] | \psi(t - \delta t_q) \rangle. \quad (87)$$

Evaluating the collapse amplitudes in $\hat{M}_{I_{\theta(t)}(t + \delta t_r)}$ yields (suppressing the time arguments for brevity),

$$\langle I_\theta | \sqrt{\kappa \Delta t} \alpha_\pm \rangle = \frac{\exp \left[-\frac{1}{2} \left(I_\theta - \sqrt{2\kappa \Delta t} \text{Re}(\alpha_\pm e^{-i\theta}) \right)^2 + i I_\theta \sqrt{2\kappa \Delta t} \text{Im}(\alpha_\pm e^{-i\theta}) - i\kappa \Delta t \text{Re}(\alpha_\pm e^{-i\theta}) \text{Im}(\alpha_\pm e^{-i\theta}) \right]}{\pi^{1/4}}. \quad (88)$$

After recalling the steady state amplitudes $\alpha_\pm = -i\sqrt{\bar{n}} \exp(\pm i \arctan(2\chi/\kappa))$ with $\bar{n} = (2\epsilon/\kappa)^2/(1 + (2\chi/\kappa)^2)$ and identifying the suitably shifted and rescaled result coordinate

$$r \equiv \frac{I_\theta}{\sqrt{\Gamma \Delta t}} + \frac{\kappa}{2\chi} \sin \theta \quad (89)$$

that involves the ensemble-average dephasing rate Γ in Eq. (84), these collapse amplitudes produce a corresponding probability distribution for r

$$p(I_\theta) dI_\theta = p(r) dr = \sqrt{\frac{\Gamma \Delta t}{\pi}} \langle \psi | \left[\exp \left(-\Gamma \Delta t (r - \cos \theta \hat{\sigma}_z)^2 \right) \otimes \hat{1} \right] | \psi \rangle dr = \langle \psi | \left[\hat{M}_r^\dagger \hat{M}_r \otimes \hat{1} \right] | \psi \rangle dr \quad (90)$$

that is a mixture of state-dependent Gaussian distributions for the result r , each centered at distinct means $\pm \cos \theta$ but with equal variance $1/2\Gamma\Delta t$, as anticipated in Eqs. (25). After reparameterization with the result coordinate r , the corresponding measurement operator takes the form,

$$\hat{M}_r \equiv (\Gamma\Delta t)^{1/4} \left[\left\langle I_\theta \left| \sqrt{\kappa\Delta t} \alpha_+ \right. \right\rangle |0\rangle\langle 0| + \left\langle I_\theta \left| \sqrt{\kappa\Delta t} \alpha_- \right. \right\rangle |1\rangle\langle 1| \right] = \sqrt{\bar{p}(r, \theta)} e^{i\omega_S \hat{\sigma}_z / 2} \hat{R}_{r, \theta}, \quad (91)$$

including a state-independent factor as expected in Eqs. (25) that cancels during renormalization,

$$\bar{p}(r, \theta) = \sqrt{\frac{\Gamma\Delta t}{\pi}} e^{-\Gamma\Delta t(r^2 + \cos^2 \theta) - 2i\Delta t \bar{\omega}(r, \theta)}, \quad \bar{\omega}(r, \theta) = \omega_S r \cos \theta - \frac{\Gamma}{4} \left(1 + \left(\frac{\kappa}{2\chi} \right)^2 \right) \sin(2\theta), \quad (92)$$

a unitary deterministic frequency shift ω_S from the ac-Stark effect in Eq. (84) that can be compensated by shifting the frequency of the rotating frame of the qubit, and the r -dependent stochastic measurement backaction $\hat{R}_{r, \theta} \in \text{SL}(2, \mathbb{C})$ anticipated in Eqs. (25) and Eq. (80).

Therefore, after choosing the appropriate rotating frame for the qubit, rescaling the observed homodyne readout I_θ to r , and partially renormalizing the state to cancel state-independent prefactors, the effective measurement backaction induced by the standard readout procedure for superconducting qubits for each time interval Δt in a sequence indeed has the form $\hat{R}_{r(t+\delta t_r), \theta(t)} \in \text{SL}(2, \mathbb{C})$ analogous to a Lorentz transformation of a point charge, as claimed. Moreover, for small Δt the distribution for the readout result r in Eq. (90) approximates a single Gaussian distribution centered at the mean value $\langle r(t+\delta t_r) \rangle = \cos[\theta(t)] \text{Tr}[\hat{\sigma}_z \hat{\rho}(t-\delta t_q)]$ determined by the expectation value of $\hat{\sigma}_z$ in the reduced qubit state $\hat{\rho}(t-\delta t_q)$ and the choice of homodyne angle $\theta(t)$, with variance $1/2\Gamma\Delta t$. A formal time-continuous limit $\Delta t \rightarrow dt$ can then approximate the observed readout as a moving-mean white-noise process,

$$\Delta t r(t + \delta t_r) \rightarrow dt r(t + \delta t_r) = dt \cos[\theta(t)] \text{Tr}[\hat{\sigma}_z \hat{\rho}(t - \delta t_q)] + dW(t + \delta t_r) / \sqrt{2\Gamma}, \quad (93)$$

where the zero-mean stochastic Wiener increment dW satisfies the Itô rule $dW^2 = dt$. Using this white-noise process limit in $\hat{R}_{r(t+\delta t_r), \theta(t)}$ for the reduced qubit state update and linearizing to construct a forward difference Itô derivative then produces the anticipated stochastic differential equation in Eq. (27).

The readout result $r(t + \delta t_r)$ depends on the (normalized) qubit state $\hat{\rho}(t - \delta t_q)$ and choice of homodyne angle $\theta(t)$ at earlier times, which is unsurprising. What is more surprising is that this more complete derivation shows that the resulting measurement backaction $\hat{R}_{r(t+\delta t_r), \theta(t)}$ still affects the qubit state $\hat{\rho}(t - \delta t_q)$ at the *earlier* time $t - \delta t_q$. Specifically, the type of conditioned evolution in $\hat{R}_{r(t+\delta t_r), \theta(t)}$ that affects the qubit state at time $t - \delta t_q$ depends on the choice of homodyne angle $\theta(t)$ made at the later time t , while the amount of backaction depends on the result $r(t + \delta t_r)$ obtained at the even-later time $t + \delta t_r$. The future choice of $\theta(t)$ will determine whether the backaction is unitary or non-unitary (hyperbolic), yielding orthogonal motions on the Bloch sphere that are readily distinguishable. This delayed choice nature of the dynamics can be (and has been) confirmed by subsequent measurements made on the qubit after observing specific records $r(t + \delta t_r)$ [21, 22, 28]. The detailed state-tracking statistics observed in these experiments are completely consistent with the retrocausal character of the effective backaction derived here. As with all delayed choice effects in quantum mechanics, however, this apparently retrocausal effect does have a more causal interpretation where the specific qubit dynamics are left indefinite as part of a joint entangled state with intrinsic uncertainty like Eq. (81) until the final collapse from observation like in Eq. (85). Nevertheless, once the specific record $r(t + \delta t_r)$ is known, the entire past history of the qubit dynamics effectively collapses to be consistent with that future record, making the retrocausal backaction $\hat{R}_{r(t+\delta t_r), \theta(t)}$ an accurate description of the effective state dynamics.

To underscore how unusual this behavior of a monitored qubit state is, despite the formal equivalence to a stochastic Lorentz transformation, consider what would have to happen to achieve equivalent dynamics

with a classical point charge according to the correspondence developed in the previous sections. The four-momentum $\hat{p}(t)$ of the charge at a time t would have to experience an external stochastic electromagnetic force,

$$\hat{p}(t + dt) = e^{\mu dt \hat{F}(t)/\hbar} \hat{p}(t) e^{\mu dt \hat{F}^\dagger(t)/\hbar}, \quad (94a)$$

$$dt \hat{F}(t) = dt \left(\hat{E}(t)/c + i \hat{B}(t) \right) = \frac{E_0}{c} \left(\cos[\theta(t + \delta t_q)] \beta_z(t) dt + dW(t + \delta t_q + \delta t_r)/\sqrt{2\Gamma} \right) e^{-i\theta(t + \delta t_q)} \hat{\sigma}_z, \quad (94b)$$

with $E_0 \mu / \hbar c = \Gamma$ such that the field explicitly depends on $\beta_z(t) = v_z(t)/c = p_z(t)/p_0(t)$, the z -component of the particle velocity ratio at time t . Such a velocity-dependent external electric field is a form of instantaneous feedback that is difficult to arrange for a classical charge. Moreover, the decomposition of the field into electric and magnetic parts would have to be determined by an experimental phase parameter $\theta(t + \delta t_q)$ that is selected a delay δt_q in the future after the field has already interacted with the particle at time t , exhibited in Fig. 4. Such a delayed choice effect is equivalent to preserving the dual-symmetry (i.e., electric-magnetic egalitarianism) of the electromagnetic field in vacuum long after the interaction with the charge [73, 74]. The choice $\theta = 0$ would produce a purely electric force in the past, while the choice $\theta = \pi/2$ would produce a purely magnetic force in the past. The fluctuations in the field $dW(t + \delta t_q + \delta t_r)$ would have to be determined even later in the future after an additional delay δt_r . This velocity dependence and temporal nonlocality that would be needed in the corresponding charge dynamics to mimic the behavior of a monitored qubit cannot be replicated by external electromagnetic fields that obey causal propagation.

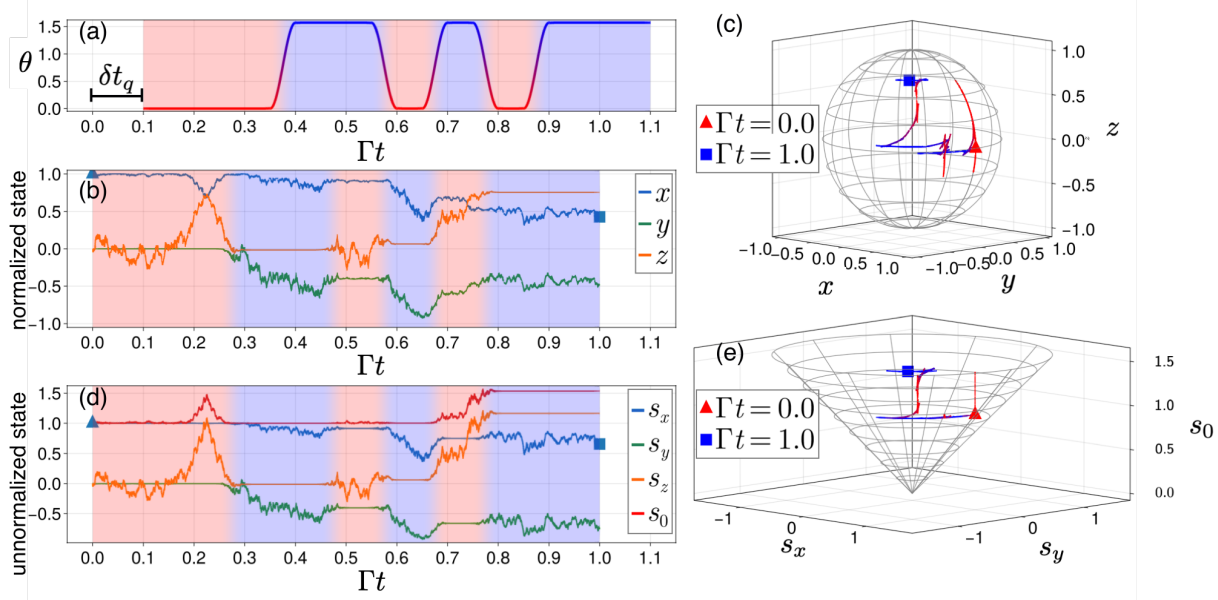


Fig. 4: Quantum trajectory simulation depicting the normalized $\hat{\rho}(t)$ and unnormalized $\hat{s}(t)$ state evolution of a continuously monitored qubit under dynamical delayed choice of the homodyne (squeezing) angle $\theta(t)$. Equivalently, one may interpret these dynamics as the (normalized) velocity $\hat{\beta}$ and (unnormalized) momentum \hat{p} evolution of a point charge in a velocity-dependent stochastic electromagnetic field with duality phase $\theta(t)$, in the form given by Eq. (94). (a) The squeezing angle is varied smoothly between informational ($\theta = 0$, red) and non-informational ($\theta = \pi/2$, blue) measurement backaction. (b) The time delay $\Gamma\delta t_q = 0.1$ between qubit and amplifier leads the choice of θ at times $t + \delta t_q$ to retroactively determine the inferred qubit dynamics at times t , as witnessed in the Bloch coordinates of the normalized state $\hat{\rho}$. (c) On the Bloch sphere, informational measurement (red) generates hyperbolic backaction between measurement eigenstates $|0\rangle$ and $|1\rangle$; non-informational measurement (blue) generates rotational backaction around $\hat{\sigma}_z$; combined informational and non-informational measurement (purple) leads to a combination of both. The initial and final states are marked by a triangle and square, respectively. (d) The unnormalized state \hat{s} shows backaction in s_z and s_0 for $\theta = 0$ and in s_x and s_y for $\theta = \pi/2$. The absence of stochasticity in the x, y components for $\theta = 0$ (red background) highlights the purely hyperbolic nature of informational backaction, which is otherwise obscured in the timeseries data of $\hat{\rho}$ by renormalization. (e) The unnormalized state lives on a four-dimensional lightcone, represented here as the s_x - s_y - s_0 slice. Noninformational backaction is visible as rotations in s_x - s_y , while informational backaction manifests as vertical motion of s_0 (s_z is not visible in this slice).

7 Conclusion

In this paper, we generalized the traditional Bloch ball representation of a normalized qubit state as a three-dimensional spin vector by lifting the normalization constraint and extending it to a proper four-vector that behaves analogously to the four-momentum of a point charge in spacetime. Crucially, this spacetime representation is faithful to the enlarged dynamical group $SL(2, \mathbb{C})$ of a monitored qubit, so can describe aspects of monitored qubit dynamics that are suppressed by the renormalized Bloch vector representation. Indeed, we showed that the Bloch three-vector corresponds in this spacetime representation to the velocity of

the corresponding charge in a particular frame, giving an interesting perspective on the apparent nonlinearity that appears in the renormalized monitored qubit dynamics. We thus expect this spacetime correspondence to be a useful visualization tool for monitored qubit dynamics that can provide intuition complementary to the Bloch ball picture.

A notable feature of the spacetime representation is that deterministic non-Hermitian dynamics are equivalent to the familiar Lorentz force on a charge generated by an electromagnetic field. This equivalence implies that the charge dynamics induced by stochastic electromagnetic fields should be able to emulate the stochastic non-Hermitian dynamics of a monitored qubit, as well as the deterministic non-Hermitian dynamics of a dissipative qubit. However, we showed that establishing the detailed correspondence to monitored qubit dynamics places unusual constraints on the fluctuating force fields: First, the stochastic electromagnetic field must depend on the velocity of the charge it is acting on, making it a fluctuating feedback-control field. Second, whether the electromagnetic field is electric or magnetic in character depends on a parameter that an experimenter can control in the future, making the type of Lorentz transformation felt by the charge a dynamical form of delayed choice. These unusual dynamical features mandated by our classical spacetime charge correspondence help clarify some of the inherent strangeness of monitored qubit evolution.

The subtle parameter dependence on the delayed future choice of an experimenter particularly highlights the inherent conceptual tension between causality and the entangled-state collapse induced by quantum measurement. We emphasize that such tension cannot be avoided in any classical hidden variable model of the measurement process, including the charge correspondence we develop here. The apparent retrocausality in our charge model thus exemplifies Carmichael's warning in Ref. [6] regarding the nature of monitored quantum trajectories: "If we adopt this [trajectory] viewpoint... we must still accept, or somehow circumvent, a manifest nonlocality in time... [The fluctuations] came from the randomness of photoelectron emissions at the detector, communicated backwards in time to the source by the collapse of the wavefunction."

Acknowledgements

We thank Alexander N. Korotkov and Andrew N. Jordan for motivating discussions regarding the Lorentz-like structure of qubit measurement and the delayed choice nature of phase-sensitive homodyne readout of superconducting qubits. This work was partially supported by the U. S. Army Research Office under grant W911NF-22-1-0258.

References

- ¹C. W. Gardiner and M. J. Collett, "Input and output in damped quantum systems: Quantum stochastic differential equations and the master equation", *Physical Review A* **31**, 3761–3774 (1985).
- ²A. Barchielli, "Measurement theory and stochastic differential equations in quantum mechanics", *Physical Review A* **34**, 1642 (1986).
- ³L. Diósi, "Continuous quantum measurement and Itô formalism", *Physics Letters A* **129**, 419–423 (1988).
- ⁴V. P. Belavkin, "Quantum continual measurements and a posteriori collapse on CCR", *Communications in Mathematical Physics* **146**, 611–635 (1992).
- ⁵J. Dalibard, Y. Castin, and K. Mølmer, "Wave-function approach to dissipative processes in quantum optics", *Physical Review Letters* **68**, 580–583 (1992).
- ⁶H. Carmichael, *An open systems approach to quantum optics: lectures presented at the Université libre de Bruxelles, October 28 to November 4, 1991*, Lecture notes in physics (Springer-Verlag, Berlin; New York, 1993).
- ⁷H. M. Wiseman and G. J. Milburn, "Quantum theory of field-quadrature measurements", *Physical Review A* **47**, 642–662 (1993).

⁸P. Goetsch and R. Graham, “Linear stochastic wave equations for continuously measured quantum systems”, *Physical Review A* **50**, 5242–5255 (1994).

⁹H. M. Wiseman, “Quantum Trajectories and Quantum Measurement Theory”, *Quantum and Semiclassical Optics: Journal of the European Optical Society Part B* **8**, arXiv:quant-ph/0302080, 205–222 (1996).

¹⁰A. N. Korotkov, “Selective quantum evolution of a qubit state due to continuous measurement”, *Physical Review B* **63**, 115403 (2001).

¹¹K. Jacobs and D. Steck, “A straightforward introduction to continuous quantum measurement”, *Contemp. Phys.* **47**, 279–303 (2006).

¹²J. Gambetta, A. Blais, D. I. Schuster, A. Wallraff, L. Frunzio, J. Majer, M. H. Devoret, S. M. Girvin, and R. J. Schoelkopf, “Qubit-photon interactions in a cavity: measurement-induced dephasing and number splitting”, *Phys. Rev. A* **74**, 042318 (2006).

¹³J. Gambetta, A. Blais, M. Boissonneault, A. A. Houck, D. I. Schuster, and S. M. Girvin, “Quantum trajectory approach to circuit QED: Quantum jumps and the Zeno effect”, *Phys. Rev. A* **77**, 012112 (2008).

¹⁴A. N. Korotkov, “Quantum Bayesian approach to circuit QED measurement”, in *Quantum Machines: Measurement and Control of Engineered Quantum Systems* (Nov. 2011), pp. 533–556.

¹⁵A. N. Korotkov, “Quantum Bayesian approach to circuit QED measurement with moderate bandwidth”, *Physical Review A* **94**, 1–24 (2016).

¹⁶H. M. Wiseman and G. J. Milburn, *Quantum measurement and control* (Cambridge University Press, 2009).

¹⁷R. Vijay, D. H. Slichter, and I. Siddiqi, “Observation of quantum jumps in a superconducting artificial atom”, *Physical review letters* **106**, 110502 (2011).

¹⁸M. Hatridge, S. Shankar, M. Mirrahimi, F. Schackert, K. Geerlings, T. Brecht, K. M. Sliwa, B. Abdo, L. Frunzio, S. M. Girvin, R. J. Schoelkopf, and M. H. Devoret, “Quantum back-action of an individual variable-strength measurement”, *Science* **339**, 178–181 (2013).

¹⁹L. Sun, A. Petrenko, Z. Leghtas, B. Vlastakis, G. Kirchmair, K. M. Sliwa, A. Narla, M. Hatridge, S. Shankar, J. Blumoff, L. Frunzio, M. Mirrahimi, M. H. Devoret, and R. J. Schoelkopf, “Tracking photon jumps with repeated quantum non-demolition parity measurements”, *Nature* **511**, 444–448 (2014).

²⁰U. Vool, S. Shankar, S. O. Mundhada, N. Ofek, A. Narla, K. Sliwa, E. Zalys-Geller, Y. Liu, L. Frunzio, R. J. Schoelkopf, S. M. Girvin, and M. H. Devoret, “Continuous Quantum Nondemolition Measurement of the Transverse Component of a Qubit”, *Physical review letters* **117**, 133601 (2016).

²¹K. W. Murch, S. J. Weber, C. Macklin, and I. Siddiqi, “Observing single quantum trajectories of a superconducting quantum bit”, *Nature* **502**, 211–214 (2013).

²²S. J. Weber, A. Chantasri, J. Dressel, A. N. Jordan, K. W. Murch, and I. Siddiqi, “Mapping the optimal route between two quantum states”, *Nature* **511**, 570–573 (2014).

²³P. Campagne-Ibarcq, P. Six, L. Bretheau, A. Sarlette, M. Mirrahimi, P. Rouchon, and B. Huard, “Observing quantum state diffusion by heterodyne detection of fluorescence”, *Phys. Rev. X* **6**, 011002 (2016).

²⁴Q. Ficheux, S. Jezouin, Z. Leghtas, and B. Huard, “Dynamics of a qubit while simultaneously monitoring its relaxation and dephasing”, *Nature Communications* **9**, 1926 (2018).

²⁵S. Hacohen-Gourgy, L. S. Martin, E. Flurin, V. V. Ramasesh, K. B. Whaley, and I. Siddiqi, “Quantum dynamics of simultaneously measured non-commuting observables”, *Nature* **538**, 491–494 (2016).

²⁶L. P. García-Pintos and J. Dressel, “Past observable dynamics of a continuously monitored qubit”, *Physical Review A* **96**, Publisher: American Physical Society, 062110 (2017).

²⁷E. Flurin, L. S. Martin, S. Hacohen-Gourgy, and I. Siddiqi, “Using a recurrent neural network to reconstruct quantum dynamics of a superconducting qubit from physical observations”, *Phys. Rev. X* **10**, 011006 (2020).

²⁸G. Koolstra, N. Stevenson, S. Barzili, L. Burns, K. Siva, S. Greenfield, W. Livingston, A. Hashim, R. Naik, J. Kreikebaum, et al., “Monitoring fast superconducting qubit dynamics using a neural network”, *Physical Review X* **12**, 031017 (2022).

²⁹R. Vijay, C. Macklin, D. H. Slichter, S. J. Weber, K. W. Murch, R. Naik, A. N. Korotkov, and I. Siddiqi, “Stabilizing Rabi oscillations in a superconducting qubit using quantum feedback”, *Nature* **490**, 77–80 (2012).

³⁰G. De Lange, D. Riste, M. Tiggelman, C. Eichler, L. Tornberg, G. Johansson, A. Wallraff, R. Schouten, and L. DiCarlo, “Reversing quantum trajectories with analog feedback”, *Physical Review Letters* **112**, 080501 (2014).

³¹T. L. Patti, A. Chantasri, L. P. García-Pintos, A. N. Jordan, and J. Dressel, “Linear feedback stabilization of a dispersively monitored qubit”, *Phys. Rev. A* **96**, 022311 (2017).

³²Z. K. Minev, S. O. Mundhada, S. Shankar, P. Reinhold, R. Gutiérrez-Jáuregui, R. J. Schoelkopf, M. Mirrahimi, H. J. Carmichael, and M. H. Devoret, “To catch and reverse a quantum jump mid-flight”, *Nature* **570**, 200–204 (2019).

³³L. S. Martin, W. P. Livingston, S. Hacohen-Gourgy, H. M. Wiseman, and I. Siddiqi, “Implementation of a canonical phase measurement with quantum feedback”, *Nature Physics* **16**, 1046–1049 (2020).

³⁴S. Hacohen-Gourgy and L. S. Martin, “Continuous measurements for control of superconducting quantum circuits”, *Advances in Physics: X* **5**, 1813626 (2020).

³⁵S. Hacohen-Gourgy, L. P. García-Pintos, L. S. Martin, J. Dressel, and I. Siddiqi, “Incoherent qubit control using the quantum Zeno effect”, *Physical review letters* **120**, 020505 (2018).

³⁶K. Kumari, G. Rajpoot, S. Joshi, and S. R. Jain, “Qubit control using quantum Zeno effect: action principle approach”, *Annals of Physics* **450**, 169222 (2023).

³⁷P. Lewalle, Y. Zhang, and K. B. Whaley, “Optimal Zeno dragging for quantum control: a shortcut to Zeno with action-based scheduling optimization”, *PRX Quantum* **5**, 020366 (2024).

³⁸S. Greenfield, L. Martin, F. Motzoi, K. B. Whaley, J. Dressel, and E. M. Levenson-Falk, “Stabilizing two-qubit entanglement with dynamically decoupled active feedback”, *Physical Review Applied* **21**, 024022 (2024).

³⁹S. Greenfield, A. Kamal, J. Dressel, and E. Levenson-Falk, “A unified picture for quantum Zeno and anti-Zeno effects”, [10.48550/arXiv.2506.12679](https://arxiv.org/abs/2506.12679) (2025).

⁴⁰N. Roch, M. E. Schwartz, F. Motzoi, C. Macklin, R. Vijay, A. W. Eddins, A. N. Korotkov, K. B. Whaley, M. Sarovar, and I. Siddiqi, “Observation of measurement-induced entanglement and quantum trajectories of remote superconducting qubits”, *Physical Review Letters* **112**, 1–5 (2014).

⁴¹A. Chantasri, M. E. Kimchi-Schwartz, N. Roch, I. Siddiqi, and A. N. Jordan, “Quantum trajectories and their statistics for remotely entangled quantum bits”, *Phys. Rev. X* **6**, 041052 (2016).

⁴²R. Mohseninia, J. Yang, I. Siddiqi, A. N. Jordan, and J. Dressel, “Always-On Quantum Error Tracking with Continuous Parity Measurements”, *Quantum* **4**, 358 (2020).

⁴³J. Atalaya, A. N. Korotkov, and K. B. Whaley, “Error-correcting Bacon-Shor code with continuous measurement of noncommuting operators”, *Phys. Rev. A* **102**, 022415 (2020).

⁴⁴Y.-H. Chen and T. A. Brun, “Continuous quantum error detection and suppression with pairwise local interactions”, *Phys. Rev. Research* **2**, 043093 (2020).

⁴⁵W. P. Livingston, M. S. Blok, E. Flurin, J. Dressel, A. N. Jordan, and I. Siddiqi, “Experimental demonstration of continuous quantum error correction”, *Nature communications* **13**, 2307 (2022).

⁴⁶N. Gisin, “A simple nonlinear dissipative quantum evolution equation”, *Journal of Physics A: Mathematical and General* **14**, 2259–2267 (1981).

⁴⁷M. B. Plenio and P. L. Knight, “The quantum-jump approach to dissipative dynamics in quantum optics”, *Reviews of Modern Physics* **70**, Publisher: American Physical Society, 101–144 (1998).

⁴⁸D. C. Brody and E.-M. Graefe, “Mixed-State Evolution in the Presence of Gain and Loss”, *Physical Review Letters* **109**, 230405 (2012).

⁴⁹A. Sergi and P. V. Giaquinta, “Linear Quantum Entropy and Non-Hermitian Hamiltonians”, *Entropy* **18**, 451 (2016).

⁵⁰S. Alipour, A. Chenu, A. T. Rezakhani, and A. del Campo, “Shortcuts to adiabaticity in driven open quantum systems: Balanced gain and loss and non-Markovian evolution”, *Quantum* **4**, 336 (2020).

⁵¹L. P. García-Pintos, S. B. Nicholson, J. R. Green, A. Del Campo, and A. V. Gorshkov, “Unifying quantum and classical speed limits on observables”, *Physical Review X* **12**, 011038 (2022).

⁵²W. Chen, M. Abbasi, B. Ha, S. Erdamar, Y. N. Joglekar, and K. W. Murch, “Decoherence-induced exceptional points in a dissipative superconducting qubit”, *Physical Review Letters* **128**, 110402 (2022).

⁵³A. S. Matsoukas-Roubeas, F. Roccati, J. Cornelius, Z. Xu, A. Chenu, and A. del Campo, “Non-Hermitian Hamiltonian deformations in quantum mechanics”, *Journal of High Energy Physics* **2023**, 1–31 (2023).

⁵⁴T. Karmakar, P. Lewalle, Y. Zhang, and K. B. Whaley, “Noise-canceling quantum feedback: non-Hermitian dynamics with applications to state preparation and magic state distillation”, [10.48550/arXiv.2507.05611](https://arxiv.org/abs/2507.05611) (2025).

⁵⁵P. M. Harrington, E. J. Mueller, and K. W. Murch, “Engineered dissipation for quantum information science”, *Nature Reviews Physics* **4**, 660–671 (2022).

⁵⁶M. Naghiloo, M. Abbasi, Y. N. Joglekar, and K. W. Murch, “Quantum state tomography across the exceptional point in a single dissipative qubit”, *Nature Physics* **15**, Publisher: Nature Publishing Group, 1232–1236 (2019).

⁵⁷Y. Ashida, Z. Gong, and M. Ueda, “Non-Hermitian physics”, *Adv. Phys.* **69**, 249–435 (2020).

⁵⁸W. Chen, M. Abbasi, Y. N. Joglekar, and K. W. Murch, “Quantum Jumps in the Non-Hermitian Dynamics of a Superconducting Qubit”, *Physical Review Letters* **127**, 140504 (2021).

⁵⁹F. Roccati, G. M. Palma, F. Bagarello, and F. Ciccarello, “Non-Hermitian physics and master equations”, *Open Systems & Information Dynamics* **29**, arXiv:2201.05367 [quant-ph], 2250004 (2022).

⁶⁰R. Wakefield, A. Laing, and Y. N. Joglekar, “Non-Hermiticity in quantum nonlinear optics through symplectic transformations”, *Applied Physics Letters* **124**, 201103 (2024).

⁶¹P. Martinez-Azcona, A. Kundu, A. Saxena, A. d. Campo, and A. Chenu, “Quantum Dynamics with Stochastic Non-Hermitian Hamiltonians”, *Physical Review Letters* **135**, 10.1103/5ks1-tjjm (2025).

⁶²Y. Aharonov, D. Z. Albert, and L. Vaidman, “How the result of a measurement of a component of the spin of a spin-1/2 particle can turn out to be 100”, *Phys. Rev. Lett.* **60**, Publisher: American Physical Society, 1351–1354 (1988).

⁶³J. Dressel, T. A. Brun, and A. N. Korotkov, “Implementing generalized measurements with superconducting qubits”, *Physical Review A* **90**, 032302 (2014).

⁶⁴J. Dressel, A. Chantasri, A. N. Jordan, and A. N. Korotkov, “Arrow of Time for Continuous Quantum Measurement”, *Physical Review Letters* **119**, Publisher: American Physical Society, 220507 (2017).

⁶⁵A. N. Jordan and A. N. Korotkov, “Qubit feedback and control with kicked quantum nondemolition measurements: A quantum Bayesian analysis”, *Physical Review B* **74**, Publisher: American Physical Society, 085307 (2006).

⁶⁶H. K. Dreiner, H. E. Haber, and S. P. Martin, “Two-component spinor techniques and Feynman rules for quantum field theory and supersymmetry”, *Physics Reports* **494**, 1–196 (2010).

⁶⁷R. Penrose and W. Rindler, *Spinors and Space-Time: Volume 1: Two-Spinor Calculus and Relativistic Fields*, Vol. 1, Cambridge Monographs on Mathematical Physics (Cambridge University Press, Cambridge, 1984).

⁶⁸D. Hestenes, “Spacetime physics with geometric algebra”, *American Journal of Physics* **71**, 691–714 (2003).

⁶⁹C. Doran, A. Lasenby, and S. Gull, “States and operators in the spacetime algebra”, *Foundations of Physics* **23**, 1239–1264 (1993).

⁷⁰C. Doran, D. Hestenes, F. Sommen, and N. Van Acker, “Lie groups as spin groups”, *Journal of Mathematical Physics* **34**, 3642–3669 (1993).

⁷¹C. Doran and A. N. Lasenby, *Geometric algebra for physicists*, 1st pbk. ed. with corr (Cambridge University Press, Cambridge ; New York, 2007).

⁷²W. E. Baylis and J. D. Keselica, “The Complex Algebra of Physical Space: A Framework for Relativity”, *Advances in Applied Clifford Algebras* **22**, 537–561 (2012).

⁷³J. Dressel, K. Y. Bliokh, and F. Nori, “Spacetime algebra as a powerful tool for electromagnetism”, *Phys. Rep.* **589**, 1–71 (2015).

⁷⁴L. Burns, K. Y. Bliokh, F. Nori, and J. Dressel, “Acoustic versus electromagnetic field theory: scalar, vector, spinor representations and the emergence of acoustic spin”, *New Journal of Physics* **22**, Publisher: IOP Publishing, 053050 (2020).

⁷⁵L. Burns, T. Daniel, S. Alexander, and J. Dressel, “Spacetime geometry of acoustics and electromagnetism”, *Quantum Studies: Mathematics and Foundations* **11**, 27–67 (2024).

⁷⁶R. Botet and H. Kuratsuji, “The duality between a non-Hermitian two-state quantum system and a massless charged particle”, *Journal of Physics A: Mathematical and Theoretical* **52**, 035303 (2019).

⁷⁷T. H. Boyer, “General connection between random electrodynamics and quantum electrodynamics for free electromagnetic fields and for dipole oscillator systems”, *Physical Review D* **11**, Publisher: American Physical Society, 809–830 (1975).

⁷⁸G. H. Goedecke, “Stochastic electrodynamics. I. On the stochastic zero-point field”, *Foundations of Physics* **13**, 1101–1119 (1983).

⁷⁹W. C.-W. Huang and H. Batelaan, “Discrete Excitation Spectrum of a Classical Harmonic Oscillator in Zero-Point Radiation”, *Foundations of Physics* **45**, 333–353 (2015).

⁸⁰P. D. Drummond and M. D. Reid, “Q-functions as models of physical reality”, *Physical Review Research* **2**, arXiv:1909.01798 [quant-ph], 033266 (2020).

⁸¹J. S. Bell, “On the Einstein Podolsky Rosen paradox”, *Physics Physique Fizika* **1**, Publisher: American Physical Society, 195–200 (1964).

⁸²H. M. Wiseman, “Steering, Entanglement, Nonlocality, and the Einstein-Podolsky-Rosen Paradox”, *Physical Review Letters* **98**, 10.1103/PhysRevLett.98.140402 (2007).

⁸³B. Wittmann, S. Ramelow, F. Steinlechner, N. K. Langford, N. Brunner, H. M. Wiseman, R. Ursin, and A. Zeilinger, “Loophole-free Einstein–Podolsky–Rosen experiment via quantum steering”, *New Journal of Physics* **14**, 053030 (2012).

⁸⁴R. Ruskov, A. N. Korotkov, and A. Mizel, “Signatures of quantum behavior in single-qubit weak measurements”, *Phys. Rev. Lett.* **96**, 200404 (2006).

⁸⁵A. N. Jordan, A. N. Korotkov, and M. Büttiker, “Leggett-Garg Inequality with a Kicked Quantum Pump”, *Phys. Rev. Lett.* **97**, 026805 (2006).

⁸⁶J. Dressel, C. J. Broadbent, J. C. Howell, and A. N. Jordan, “Experimental Violation of Two-Party Leggett–Garg Inequalities with Semiweak Measurements”, *Phys. Rev. Lett.* **106**, 040402 (2011).

⁸⁷J. Dressel and A. N. Korotkov, “Avoiding loopholes with hybrid Bell-Leggett-Garg inequalities”, *Phys. Rev. A* **89**, 012125 (2014).

⁸⁸T. C. White, J. Y. Mutus, J. Dressel, J. Kelly, R. Barends, E. Jeffrey, D. Sank, A. Megrant, B. Campbell, Y. Chen, Z. Chen, B. Chiaro, A. Dunsworth, I.-C. Hoi, C. Neill, P. J. J. O’Malley, P. Roushan, A. Vainsencher, J. Wenner, A. N. Korotkov, and J. M. Martinis, “Preserving entanglement during weak measurement demonstrated with a violation of the Bell–Leggett–Garg inequality”, *npj Quant. Inf.* **2**, 15022 (2016).

⁸⁹R. W. Spekkens, “Contextuality for preparations, transformations, and unsharp measurements”, *Physical Review A* **71**, arXiv: quant-ph/0406166, 052108 (2005).

⁹⁰R. W. Spekkens, “Evidence for the epistemic view of quantum states: A toy theory”, *Phys. Rev. A* **75**, 032110 (2007).

⁹¹G. Chiribella and R. W. Spekkens, eds., *Quantum Theory: Informational Foundations and Foils*, Vol. 181, Fundamental Theories of Physics (Springer Netherlands, Dordrecht, 2016).

⁹²E. T. Jaynes and G. L. Bretthorst, *Probability theory: the logic of science* (Cambridge university press, Cambridge, 2003).

⁹³Z.-Q. Zhou, S. F. Huelga, C.-F. Li, and G.-C. Guo, “Experimental Detection of Quantum Coherent Evolution through the Violation of Leggett-Garg-Type Inequalities”, *Physical Review Letters* **115**, 113002 (2015).

⁹⁴K. Jacobs and D. A. Steck, “A straightforward introduction to continuous quantum measurement”, *Contemporary Physics* **47**, 279–303 (2006).

⁹⁵Z. Shangnan and Y. Wang, *Quantum Cross Entropy and Maximum Likelihood Principle*, Oct. 2022.

⁹⁶K. W. Murch, S. J. Weber, C. Macklin, and I. Siddiqi, *Observing single quantum trajectories of a superconducting qubit*, arXiv:1305.7270, Oct. 2013.

⁹⁷J. Koch, T. M. Yu, J. Gambetta, A. A. Houck, D. I. Schuster, J. Majer, A. Blais, M. H. Devoret, S. M. Girvin, and R. J. Schoelkopf, “Charge-insensitive qubit design derived from the cooper pair box”, *Phys. Rev. A* **76**, 042319 (2007).

Appendix

Here we derive the stochastic increments for both unnormalized \hat{p} and normalized $\hat{\beta}$ states. Consider stochastic transformations of the form $\hat{R} = \exp(\lambda dt \hat{F})$ where $\hat{F} = \hat{F}_D + \hat{F}_\xi$, and $dt \hat{F}_\xi = \sum_j dW_j \hat{F}_j$ with $(dW_j)^2 = dt$. We obtain

$$\hat{p}(t + dt) = \hat{R} \hat{p} \hat{R}^\dagger = \left(1 + \lambda dt \hat{F} + \frac{(\lambda dt \hat{F}_\xi)^2}{2} \right) \hat{p}(t) \left(1 + \lambda dt \hat{F}^\dagger + \frac{(\lambda dt \hat{F}_\xi^\dagger)^2}{2} \right) + O(dt^{3/2}), \quad (95)$$

which yields the stochastic momentum increment

$$d\hat{p} = \hat{R} \hat{p} \hat{R}^\dagger - \hat{p} = \lambda \left(dt \left\{ \hat{F}_D, \hat{p} \right\} + \frac{\lambda}{2} \left\{ dt \hat{F}_\xi, \left\{ dt \hat{F}_\xi, \hat{p} \right\} \right\} \right) + \lambda \left\{ dt \hat{F}_\xi, \hat{p} \right\} + O(dt^{3/2}) \approx d\hat{p}_D + d\hat{p}_\xi, \quad (96)$$

the first term deterministic, order dt , and the second term is stochastic, order dW , with anticommutator defined as $\{A, B\} = AB + BA^\dagger$. The equation for the unnormalized qubit state \hat{s} is identical, with $\hat{H}_{\text{eff}} = i\lambda \hat{F}$.

The dynamics obeyed by $\hat{\beta} = \hat{p} / \text{Tr } \hat{p}$, can be derived as follows. To first order in dW and dt , we expand

$$\frac{1}{\text{Tr } \hat{p} + \text{Tr}(d\hat{p})} = \frac{1}{\text{Tr } \hat{p}} - \frac{\text{Tr}(d\hat{p})}{(\text{Tr } \hat{p})^2} + \frac{\text{Tr}(d\hat{p})^2}{(\text{Tr } \hat{p})^3} + O(dt^{3/2}) \quad (97)$$

and write

$$\hat{\beta}(t + dt) = \frac{\hat{p}(t) + d\hat{p}(t)}{\text{Tr } \hat{p}(t) + \text{Tr}(d\hat{p}(t))} = \hat{\beta} + \frac{d\hat{p}}{\text{Tr } \hat{p}} - \frac{\hat{\beta} \text{Tr}(d\hat{p})}{\text{Tr } \hat{p}} - \frac{\text{Tr}(d\hat{p})}{\text{Tr } \hat{p}} \left(\frac{d\hat{p}}{\text{Tr } \hat{p}} - \frac{\hat{\beta} \text{Tr}(d\hat{p})}{\text{Tr } \hat{p}} \right) + O(dt^{3/2}), \quad (98)$$

finding

$$d\hat{\beta} = \frac{d\hat{p}}{\text{Tr } \hat{p}} - \frac{\hat{\beta} \text{Tr}(d\hat{p})}{\text{Tr } \hat{p}} - \frac{\text{Tr}(d\hat{p})}{\text{Tr } \hat{p}} \left|_{dW} \right. \left(\frac{d\hat{p}}{\text{Tr } \hat{p}} - \frac{\hat{\beta} \text{Tr}(d\hat{p})}{\text{Tr } \hat{p}} \right) \left|_{dW} \right. + O(dt^{3/2}) \approx d\hat{\beta}_D + d\hat{\beta}_\xi. \quad (99)$$

The stochastic part of the velocity update

$$d\hat{\beta}_\xi = \lambda \left(\left\{ dt \hat{F}_\xi, \hat{\beta} \right\} - \text{Tr} \left(\left\{ dt \hat{F}_\xi, \hat{\beta} \right\} \right) \hat{\beta} \right) \quad (100)$$

is identical to the innovation term of the stochastic master equation for the normalized density matrix \hat{p} . The Itô correction takes the form,

$$\frac{\text{Tr}(d\hat{p})}{\text{Tr } \hat{p}} \left|_{dW} \right. \left(\frac{d\hat{p}}{\text{Tr } \hat{p}} - \frac{\hat{\beta} \text{Tr}(d\hat{p})}{\text{Tr } \hat{p}} \right) \left|_{dW} \right. = \lambda^2 \text{Tr} \left(\left\{ dt \hat{F}_\xi, \hat{\beta} \right\} \right) \left(\left\{ dt \hat{F}_\xi, \hat{\beta} \right\} - \text{Tr} \left(\left\{ dt \hat{F}_\xi, \hat{\beta} \right\} \right) \hat{\beta} \right), \quad (101)$$

and contributes to the deterministic increment,

$$d\hat{\beta}_D = \lambda \left(\left\{ dt \hat{F}'_D, \hat{\beta} \right\} - \text{Tr} \left(\left\{ dt \hat{F}'_D, \hat{\beta} \right\} \right) \hat{\beta} \right) + \lambda^2 \left(dt \hat{F}_\xi \hat{\beta} dt \hat{F}_\xi^\dagger - \text{Tr} \left(dt \hat{F}_\xi \hat{\beta} dt \hat{F}_\xi^\dagger \right) \hat{\beta} \right) \quad (102)$$

where the Itô correction modifies the effective deterministic generator of motion

$$dt \hat{F}'_D = dt \hat{F}_D - \lambda \text{Tr} \left(\left\{ dt \hat{F}_\xi, \hat{\beta} \right\} \right) dt \hat{F}_\xi. \quad (103)$$

The same dynamics govern the normalized qubit state $\hat{\rho}$ under identification between effective electromagnetic field and effective non-Hermitian generator, $dt \hat{H}'_{\text{eff}} = i\lambda dt \hat{F}' = i\lambda(dt \hat{F}'_D + dt \hat{F}_\xi)$.